The Apparent Partitioning Behaviour of SARS-CoV-2 RNA in Municipal Wastewater

by

Patrick Raymond Breadner

A thesis

presented to the University of Waterloo

in fulfillment of the

thesis requirement for the degree of

Master of Science

in

Biology (Water)

Waterloo, Ontario, Canada, 2023

Author’s Declaration

I hereby declare that I am the sole author of this thesis. This is a true copy of the thesis, including any required final revisions, as accepted by my examiners.

I understand that my thesis may be made electronically available to the public.

Abstract

The use of wastewater-based surveillance (WBS) has experienced rapid expansion and development since the onset of the coronavirus disease (COVID-19) pandemic that is caused by the virus severe acute respiratory syndrome coronavirus 2 (SARS-CoV-2). WBS has become a vital resource for tracking the spread of COVID-19 across communities as fragments of SARS-CoV-2 RNA can be quantified and measured temporally in wastewater. However, the absence of standardized methods across labs and remaining methodological issues can impact the interpretation of data for public health efforts. In particular, characterizing how RNA fragments of SARS-CoV-2 partition in wastewater is a central part of understanding its fate and behaviour in the wastewater. Additionally, various laboratories analyze either the liquid or solid fraction, and this has implications for the interpretation of analytical results and trends. The partitioning of SARS-CoV-2 RNA was examined in a series of experiments that were conducted using centrifugation with varied spin time and centrifugal force, polyethylene glycol precipitation followed by centrifugation, and ultrafiltration of wastewater. Partitioning of the endogenous pepper mild mottled virus (PMMoV) was also examined as it is commonly used to normalize the SARS-CoV-2 signal for fecal load in trend analysis. Additionally, two coronavirus surrogates, human coronavirus 229E and murine hepatitis virus, were analyzed as internal process controls. Although SARS-CoV-2 has an affinity for solids, the total RNA copies of SARS-CoV-2 per wastewater sample split evenly between the liquid and solid fractions after centrifugation (i.e., 12,000 x *g* for 1.5 h without a brake). A longer and faster spin resulted in a shift in partitioning for all viruses toward the solid fraction except for PMMoV which remained mostly in the liquid fraction. This observation supports that the surrogates are more reflective of SARS-CoV-2 than the endogenous reference (PMMoV). Surprisingly, ultrafiltration devices were inconsistent in estimating RNA copies in wastewater which can influence the interpretation of partitioning. Developing a better understanding of the fate of SARS-CoV-2 in wastewater and creating a foundation of best practices is key to supporting the current pandemic response but also to prepare for future potential infectious diseases.

Acknowledgements

I would first like to thank my supervisor, Dr. Mark Servos, for his exceptional guidance and support. I frequently think back to our first conversation and am tremendously appreciative of where I have been able to grow since then. Throughout my master's, Dr. Servos has been a wonderful supervisor and I have thoroughly enjoyed the spontaneous discussions about running the next series of experiments. I would also like to thank my committee, Dr. Paul Craig and Dr. Brain Dixon, for their thoughtful insight and feedback to help me improve upon my work.

Thank you to all the members of the Servos Lab with special thanks to Hadi Dhiyebi and Leslie Bragg for their continued support throughout my time as a member of the lab. Thank you, Nivetha Srikanthan and Samina Hayat for your vote of confidence and assistance in experimental planning. Finally, thank you to the many members of the lab that have assisted with my lab work and with the welcomed invitations to assist in their field/lab work. The collaborative nature of the Servos Lab is something I will always cherish and aim to bring with me moving forward.

It would not have been possible to conduct a substantial portion of my research without the viral surrogates, human coronavirus 229E and murine hepatitis virus, that were cultured and provided by Dr. Marc Aucoin and Ph.D. candidate Scott Joseph Boegel. Additionally, the qPCR assay development by the Servos Lab for its COVID-19 wastewater program has made it possible for me to accomplish the necessary lab work for my thesis.

A final thank you to my partner Taylor, family, and friends for their continued support and love during my time as a student. My success would not be possible without you.

Table of Contents

List of Figures

List of Tables

Chapter 1
General Introduction

1.1 COVID-19 and its Emergence

Coronavirus disease (COVID-19) is an upper respiratory disease caused by the virus severe acute respiratory syndrome coronavirus 2 (SARS-CoV-2) and can present itself through various symptoms including fever or chills, coughing, sore throat, diarrhea, loss of taste or smell, and others (Centers for Disease Control and Prevention [CDC], 2022b). Commonly compared to influenza, symptoms alone cannot differentiate COVID-19 from it and a PCR test is required to discern between the two (CDC, 2022b). A potential prognosis of COVID-19 is the development of post-COVID condition (PCC) which is also commonly known as "long COVID" (CDC, 2022c). PCC has a working definition of signs, symptoms, and conditions that develop during or following the inflection of COVID-19 that persist for longer than four weeks. PCC is not one condition and can be multisystemic lasting for an unknown period of time with the possibility of reoccurrence after apparent recovery. Possible PCC symptoms my include chest pain, coughing, sleep problems, depression or anxiety, as well as many others (CDC, 2022c). Of note, approximately one-third of cases experience persistent fatigue and over one-fifth of cases experience cognitive impairment 12 or more weeks after their COVID-19 diagnosis (Ceban et al., 2022). There continues to be research into PCC as more data becomes available as COVID-19 and PCC, therefore, represent a major threat to public health around the globe.

On December 31, 2019, cases of "pneumonia of unknown etiology" were reported to the World Health Organization (WHO) China County Office in Wuhan City, Hubei Province of China originating from the Huanan Seafood market (WHO, 2020a). By January 1, 2020, the national authorities in China reported 44 cases to the WHO with 121 close contacts identified (WHO, 2020a). On January 9, 2020, the causes of the cases were identified to be the result of a novel coronavirus (2019-nCoV, renamed to COVID-19) (WHO, 2020b) and by March 11, 2020, the WHO announced that COVID-19 was a global pandemic (WHO, 2020c). The spread of COVID-19 was rapid as countries struggled to contain the spread of the virus and grapple with imposing public health measures. Within one year of COVID-19's emergence, rapid advances in vaccine development allowed for widespread vaccination programs that have reduced caseloads, hospitalizations and deaths; although, vaccines have been mostly administered in first-world nations (United Nations, 2021). Globally, vaccination rates have plummeted since December 2021 (Mathieu et al., 2020, 2021). Three years since the onset of the pandemic, the effects around the globe continue to be felt and each country's ability to contain the virus has been challenged by the emergence of

new variants that affect COVID-19's transmissibility and virulence, vaccine efficacy (CDC, 2022a), vaccine hesitancy (Roy et al., 2022), and disinformation regarding the pandemic (van Mulukom et al., 2022).

There have been more than 4.4 M reported cases in Canada (as of Dec. 13, 2022) with approximately 11,000 cases per 100,000 individuals across the country (Government of Canada, 2022). Moreover, the transmission of the virus in northern, remote, and isolated communities in Canada has been a major concern due to non-equitable access to health care and testing (Respiratory Virus Infections Working Group, 2020). Throughout the pandemic, Canada has implemented a variety of methods/tools to combat the virus, including social distancing and mask mandates, capacity limits at stores and other establishments, lockdowns, and vaccine rollout. However, in light of this, few measures remain in place to limit the spread of COVID-19 as mask mandates and travel restrictions have been removed. Up until the Omicron wave (Dec. 2021), clinical testing has played an important role in informing public health decisions. With the onset of the Omicron variant, testing facilities were inundated with individuals positive for COVID-19 which led to changes in testing eligibility that reduced clinical testing reliability as a metric to gauge COVID-19 prevalence in a community. Throughout the pandemic, wastewater-based surveillance (WBS), which is independent of clinical testing, has emerged as an effective approach for community surveillance of SARS-CoV-2.

1.2 Wastewater-Based Surveillance

Wastewater-based surveillance is a growing field of science that has many applications, including monitoring antimicrobial resistance (Hendriksen et al., 2019), population drug use (Castiglioni et al., 2013), and pathogens. Success has been achieved in tracking past virus eradication campaigns for polio (Lago et al., 2003), and monitoring other infectious diseases, including hepatitis, norovirus (Hellmer et al., 2014), and influenza (Heijnen & Medema, 2011). On March 4/5, 2020, the first detection of SARS-CoV-2 RNA in wastewater was observed in the Netherlands (Medema et al., 2020). Since then, wastewater-based surveillance for COVID-19 has expanded rapidly around the globe with an emphasis on it serving as a complementary tool for Public Health Units (PHUs) (Aguiar-Oliveira et al., 2020; Hrudey et al., 2020).

Wastewater surveillance for COVID-19 is particularly valuable due to its independence from clinical testing of individuals and inclusion of asymptomatic individuals, and it also has the advantage of being free of biases associated with race, gender, age, or financial means (Safford et al., 2022; WHO, 2022).

When a person contracts COVID-19, SARS-CoV-2 RNA can be detected in multiple clinical specimens, including saliva, urine, naso/oropharyngeal swabs, and feces (Jeong et al., 2020). Some of the viral fragments enter the wastewater and monitoring of the sewer or influent of treatment plants have been effective at detecting SARS-CoV-2 viral fragments. Community monitoring can be both large-scale (wastewater treatment plants, pumping stations) or small-scale (hospitals, long-term care homes, schools), providing snapshots of COVID-19 in the community that is associated within that sewershed. Through frequent sampling, a longitudinal wastewater dataset can be created that closely reflects trends in clinical cases in many different communities (Manuel et al., 2022; Medema et al., 2020; Wurtzer et al., 2022). Wastewater surveillance for COVID-19 bridges the gap between the population of the total number of infected individuals and diagnostic metrics such as clinical testing, hospitalizations, intensive care occupancy, and so forth as it is not influenced by the aforementioned biases observed by said metrics (World Health Organization, 2022). Thus, it is a valuable and supporting indicator of the prevalence of COVID-19 in a sampled region.

Several municipalities in Canada have implemented COVID-19 WBS with government or university partners as a way to inform public health decisions. Several Canadian interlaboratory studies have been conducted to share experiences, improve, and compare the performance of methods (Canadian Water Network, 2020; Chik et al., 2021; Hrudey et al., 2022). In Ontario, the Ministry of Environment, Conservation and Parks (MECP) has created a network of university-based labs and PHUs to conduct wastewater surveillance of SARS-CoV-2 called the Wastewater Surveillance Initiative (WSI) (MECP, 2022). National collaboration between local PHUs, governments, academia, and private research labs has contributed to the success of WBS in Canada (Hrudey et al., 2022). As early as March 2020, several Canadian labs pivoted their existing research programs to the environmental surveillance of SARS-CoV-2 to support public health agencies and PHUs faced with responding to the COVID-19 pandemic (Hrudey et al., 2022). The analytical methods applied to detect the virus fragments in wastewater have varied considerably across studies (Chik et al., 2021; Pecson et al., 2021). Although this surveillance has been a success, there remains a need to further improve, adapt, and validate the analytical methods as new knowledge emerges. Our understanding of the fate and behaviour of the SARS-CoV-2 viral fragments is still very poor but critical for method development and interpretation of the data being reported.

1.3 Viral RNA Partitioning

A myriad of challenges exists across every step of quantifying SARS-CoV-2 RNA in wastewater. Inter- and intra-sample variability, as well as SARS-CoV-2 partitioning behaviour (liquid vs solid fraction), can leave uncertainty and reduce confidence in individual data. Despite these challenges, there is a strong relationship between the wastewater signal and reported clinical cases in communities (Manuel et al., 2022; Medema et al., 2020; Wurtzer et al., 2022). To further improve the interpretation of wastewater results, upstream factors such as fecal load and sewershed dilution have been considered (D'Aoust et al., 2021; Wu et al., 2020). Pepper mild mottled virus (PMMoV) is an enteric virus widely distributed in wastewaters (Kitajima et al., 2018) that has been commonly used to normalize for fecal load (Aguiar-Oliveira et al., 2020; Chik et al., 2021; D'Aoust et al., 2021; Wu et al., 2020). The gene copies per volume of SARS-CoV-2 are divided by gene copies per volume of PMMoV to normalize the data. Under some conditions, this has been found to better define SARS-CoV-2 RNA trends as PMMoV normalization can reduce variation that exists from within the sewershed or from sample analysis itself (D'Aoust et al., 2021). However, in other contexts, normalization with PMMoV has not had the same improvement for SARS-CoV-2 RNA trends (Ai et al., 2021; Dhiyebi et al., 2023b; Feng et al., 2021). There are, however, numerous other biomarkers in wastewater that can be used as an endogenous control to normalize against. Other biomarkers may include but are not limited to cross-assembly phage (crAssphage) (Ai et al., 2021), human *Bacteroides* HF183 (Feng et al., 2021), or various chemical compounds such as caffeine or paraxanthine (Hsu et al., 2022). Each of these is unique and has benefits and drawbacks to consider when being used to normalize a trend of SARS-CoV-2 RNA in wastewater. Regardless, a great challenge for WBS programs is the inherent variability that exists in the wastewater sample and solutions may only be context/system dependent.

The partitioning of SARS-CoV-2 in wastewater can be described as the amount of virus that is associated with the solid fraction and the amount of virus that is in the liquid fraction; together representing the whole wastewater sample. A key consideration to recognize is that the liquid fraction may contain solids that were not removed from the liquid fraction during separation processes such as centrifugation (Basha, 2020; Leung, 2020). Factors such as particle size, particle density, liquid density, and liquid viscosity affect how solids are settled out of solution during centrifugation (Basha, 2020). Additionally, the concentration and aggregation of solids contribute to settling dynamics during centrifugation (Leung, 2020). Using a centrifugation-based approach, the resulting pellet represents the

"solid fraction," and the supernatant represents the "liquid fraction." Of course, there is the caveat that the pellet is a "wet pellet," and the supernatant contains some non-settled solids as described above.

To further concentrate the RNA from the supernatant (liquid), a common approach is through ultrafiltration. For filtration, membrane size sets the limit for the size of solids that may remain in the liquid fraction (e.g., a pore size of 50 µm). Ultrafiltration is a membrane separation process that includes microfiltration (Aptel & Clifton, 1986). After centrifugation to remove large particles, the resulting liquid phase ("centrate") is passed through the membrane under pressure and it excludes particles of a selected size (e.g., 10 kDa). The flowthrough is referred to as the "filtrate" and the remaining liquid is referred to as the "concentrate." The virus particles are either too large to pass through or are bound to particles that cannot pass through the membrane. These ultrafiltration devices can vary in shape (Figure A1) and characteristics (Table A1), but the principle remains the same. Finally, methods such as polyethylene glycol (PEG) precipitation followed by centrifugation can be used to capture RNA from both the solid and liquid fractions of the wastewater. This method has been used for several decades to concentrate viruses (Shieh et al., 1995). The PEG precipitation method facilitates viral concentration through the steric exclusion of H_2O thereby coagulating viral material into flocs that are more readily pelleted (Atha & Ingham, 1981; Poison, 1977). Overall, these methods set out to accomplish the same goal, to concentrate the viral material from a wastewater sample before extracting the RNA.

Initially, in the development of methods for SARS-CoV-2, many researchers targeted the liquid fraction (after filtration or slow centrifugation) of wastewater (Medema et al., 2020; Wu et al., 2020), while others found success by focusing on the solid fraction (D'Aoust et al., 2021). It is evident based on many studies, including the Canadian interlaboratory study (Canadian Water Network, 2020; Chik et al., 2021), that both fractions contain SARS-CoV-2 RNA as both centrifugation and ultrafiltration methods have been successful. However, the partitioning among the various phases has not been well explored. The envelope structure of SARS-CoV-2 has been proposed to be a contributing factor for its solid fraction association compared to other viruses such as PMMoV which lacks an envelope (Ahmed et al., 2020; Kitamura et al., 2021). Furthermore, if wastewater samples are frozen before analysis, either purposefully or by environmental conditions during transportation, the effect of freezing on the signal and partitioning needs to be considered. For example, freezing a wastewater sample may disproportionally affect the liquid fraction compared to the solid fraction (Markt et al., 2021; Simpson et al., 2021) due to crystal formation that shears the RNA (Michael-Kordatou et al., 2020; Röder et al., 2010). With that in mind, there is evidence that wastewater can be held for up to a week without major RNA losses (Hokajärvi et

al., 2021; Islam et al., 2022; Simpson et al., 2021). Thus, to avoid introducing biases to the fate of viruses in wastewater by using frozen samples, fresh influent is ideal for experimentation. Overall, the fate of the virus and the RNA fragments in wastewater is still not well understood despite the importance it may have on the detection of methods and interpretation of surveillance trends.

1.4 Surrogates

Process surrogates play an important role in the analytical analysis and study of the behaviour of particles, substances, and organisms in the environment (McCarty & Aieta, 1984; Sinclair et al., 2012). They can be used as process controls (QA/QC) or potentially be used to model the analyte of interest under different experimental conditions (Sinclair et al., 2012). To be effective, the surrogate must reflect the same environmental behaviour of the analyte of interest (such as SARS-CoV-2) (Sinclair et al., 2012). Many viruses have been applied to COVID-19 wastewater surveillance as process surrogates, including human coronavirus 229E (229E) (D'Aoust et al., 2021), murine hepatitis virus (MHV) (Ahmed et al., 2020), human coronavirus OC43 (OC43) (Philo et al., 2021), bovine coronavirus (BCoV), bacteriophage MS2 (MS2), and pseudomonas phage phi6 (φ6) (Pecson et al., 2021). However, there may be many differences in the fate and behaviour of these viruses compared to SARS-CoV-2 and these differences can impact the use and interpretation of results when applied as a surrogate. Although PMMoV has been widely used as a fecal indicator in wastewater (internal endogenous control), it is morphologically different than SARS-CoV-2 and it may also have different properties that influence its fate in wastewater (LaTurner et al., 2021). A layered approach, both with an internal endogenous control (e.g., PMMoV) and a process surrogate (e.g., 229E) is important to assess potential sources for inter- and intra- sample variation. Unfortunately, process surrogates under some situations have been found to not directly reflect the fate of SARS-CoV-2 (Chik et al., 2021). This has limited the use of process surrogates and research on how these surrogates could be best applied under various conditions remains lacking.

Surrogates can be a viable option to indirectly explore the fate of SARS-CoV-2. Selecting a surrogate that is similar to SARS-CoV-2 attempts to mitigate potential confounding factors that may arise from using a dissimilar virus. For example, 229E and MHV are coronaviruses (family Coronaviridae) like SARS-CoV-2 (International Committee on Taxonomy of Viruses, 2021). As coronaviruses, they share an enveloped membrane and are positive-strand RNA viruses (Artika et al., 2020). Before methods were established to measure SARS-CoV-2 RNA in wastewater, several studies had previously used surrogates to better document the behaviour of viruses in water and wastewater (Aguado et al., 2019; Aquino De

Carvalho et al., 2017; Casanova et al., 2009; Ye et al., 2016). These earlier studies acted as a starting point to develop methods to measure SARS-CoV-2 RNA in wastewater. It is, however, important to validate the surrogates using real wastewater. Although SARS-CoV-2 itself (heat-inactivated, synthetic, shielded, etc.) could be added and compared to the surrogate that was added at the same time to the sample, there would need to be a very low SARS-CoV-2 signal to allow for the detection of the added SARS-CoV-2 material and to not confound the interpretation. Securing a sample with very low SARS-CoV-2 concentrations in wastewater to conduct experiments is not simple as the sample would need to be collected fresh during a period when concentrations are very low (near or below the limit of quantification). Since the emergence of the Omicron variant in late 2021, SARS-CoV-2 RNA signals simply have not dropped this low in many regions. Despite this, endogenous SARS-CoV-2 and added surrogates can still be compared in partitioning experiments. These methods need to be validated carefully to ensure the surrogates reflect the behaviour of SARS-CoV-2 in real wastewater.

1.5 Research Goals

The goal of the thesis is to (1) characterize the partitioning behaviour of SARS-CoV-2 and PMMoV in municipal wastewater using different approaches and (2) compare the behaviour of seeded surrogates (229E and MHV) in relation to SARS-CoV-2 in wastewater. The goal of this research is to inform the wastewater-based surveillance of COVID-19 to allow for better methods and interpretation of results. The work will help to ensure better WBS methods and approaches for future surveillance of emerging infectious diseases. The tested null hypothesis is:

- H_0: The partitioning of SARS-CoV-2 in wastewater is the same as the surrogates (229E, MHV) or the internal endogenous reference (PMMoV).

During the early pandemic, it was recognized that process controls (surrogates) were needed to assess the methods being developed and to document the recovery of SARS-CoV-2 in wastewater. However, supply issues restricted what was available and a diverse number of methods were developed quickly. Some of these early methods focused on ultrafiltration (Ahmed et al., 2020; Torii et al., 2021) but as previously mentioned, the availability of ultrafiltration devices was limited early on in the pandemic so alternative methods were developed. These were focused on the precipitation of solids and RNA using

polyethylene glycol (PEG) and/or centrifugation of the solids at different speeds. In the University of Waterloo lab, an overnight PEG precipitation method was developed followed by centrifugation at 12,000 x *g* for 1.5 h (without a brake) and has become the routine method for surveillance of several sites across Ontario. Since the spring of 2020, there have been seven waves of COVID-19 (Public Health Ontario, 2023). During this period, several experiments were designed to explore the partitioning of SARS-CoV-2, PMMoV, and two surrogates (229E and MHV) in fresh wastewater. During each of the experiments, a similar approach was used to determine the apparent partitioning of these endpoints in wastewater using the tools available at the time. In each experiment, ultrafiltration (different devices as available) and different centrifugal conditions were applied to better understand the fate of the viruses and to allow for better methods and interpretation of surveillance results. The experiment was repeated four times during the pandemic with fresh influent and slight differences in the methods, including different ultrafiltration devices (as available) as described above. The results were consistently compared to the method (overnight PEG precipitation/centrifugation) being used in the University of Waterloo SARS-CoV-2 wastewater surveillance program.

Chapter 2
The Apparent Partitioning Behaviour of SARS-CoV-2 RNA in Municipal Wastewater

2.1 Introduction

Wastewater-based surveillance (WBS) has emerged as an important tool in supporting Public Health Units (PHUs) during the COVID-19 pandemic (Hrudey et al., 2022). As people contract COVID-19, they shed viral RNA fragments of SARS-CoV-2 in their feces that can enter the municipal wastewater sewer systems. These RNA fragments can then be quantified over time to track trends in the amount of COVID-19 infections in a community (Medema et al., 2020). A key advantage of WBS is its broad-stroke approach to community-level surveillance and its independence of clinical testing including symptomatic and asymptomatic individuals. It is not affected by socioeconomic factors that can impact seeking behaviour or access to clinical testing and bias results for vulnerable populations (Safford et al., 2022; WHO, 2022). Furthermore, it can be adapted for congregate settings such as long-term care homes, prisons, and schools as well as northern, remote, and isolated communities (Hrudey et al., 2022; Manuel et al., 2022; Respiratory Virus Infections Working Group, 2020). In Ontario, Canada, the utility of WBS has become especially important for PHUs as clinical testing eligibility was restricted at the end of 2021 with the emergence of the Omicron variant. WBS has the potential to be an important tool beyond the COVID-19 pandemic as already demonstrated by its use for influenza, respiratory syncytial virus, and other respiratory viruses (Boehm et al., 2022; Hughes et al., 2022; Mercier et al., 2022)

Despite the expansion of WBS during the COVID-19 pandemic, there has not yet been a standardization of methods that measure SARS-CoV-2 RNA in wastewater. Many concentration approaches have been used to measure SARS-CoV-2 RNA in wastewater to varying effectiveness. Some of these methods include direct capture of the solids following centrifugation or ultracentrifugation, ultrafiltration, electronegative membrane adsorption, and polyethylene glycol (PEG) precipitation (La Rosa et al., 2020). In principle, these all set out to achieve the same goal to isolate and concentrate viral RNA from a wastewater sample. However, they do not necessarily provide equivalent estimates of SARS-CoV-2 RNA in wastewater (Chik et al., 2021; Pecson et al., 2021) as they are fundamentally different in their approach. The ultrafiltration methods usually concentrate virus using a membrane of a selected size (usually after centrifugation or filtration to remove the large particles). A centrifugation method uses

centrifugal force and is sometimes combined with chemicals (e.g., PEG and NaCl) to facilitate aggregation/precipitations to form a pellet. Typically, the selected methods ignore the virus that exists in the other phase. Despite the lack of standardization and the application of diverse methods, WBS for SARS-CoV-2 RNA has been shown to correlate to COVID-19 clinical cases in many communities (Manuel et al., 2022; Medema et al., 2020; Wurtzer et al., 2022).

Partitioning behaviour is an important aspect to consider with respect to estimating viral RNA concentrations in wastewater. Concentration methods have targeted the solid fraction (e.g., pelleted solids post centrifugation), the liquid fraction (e.g., concentrate from ultrafiltration), or both the liquid and solid fraction together (e.g., PEG precipitation with or without centrifugation) (Chik et al., 2021; Pecson et al., 2021). Both liquid-based (Medema et al., 2020; Wu et al., 2020) and solid-based (D'Aoust et al., 2021; Kitamura et al., 2021) methods have found success with quantifying SARS-CoV-2 RNA in wastewater despite focusing on different phases. However, there has been an increasing preference toward solid-based approaches in the literature (Chik et al., 2021; D'Aoust et al., 2021; Graham et al., 2021; Kim et al., 2022; Kitamura et al., 2021). While it is clear that SARS-CoV-2 RNA is strongly associated with the solids fraction (Kim et al., 2022), the fact that ultrafiltration methods can also be used to quantitate and track trends of the SARS-CoV-2 RNA signal suggest that a large portion remains in the liquid fraction. Overall, the partitioning of SARS-CoV-2 RNA and how methods fundamentally measure it can affect the interpretation of surveillance data.

Ideally, a surrogate would be used that has a similar partitioning behaviour as SARS-CoV-2 in wastewater to estimate recovery and monitor the performance of the method. Unfortunately, the use of surrogates has been challenging. The human coronavirus 229E (229E) and murine hepatitis virus (MHV), which are closely related to SARS-CoV-2 in the Coronaviridae family (International Committee on Taxonomy of Viruses, 2021), have been used as SARS-CoV-2 surrogates in other studies (Ahmed et al., 2020; Graham et al., 2021; Islam et al., 2022; Mondal et al., 2021). Due to their morphological similarities (e.g., enveloped membrane, positive-strand RNA, spherical shape with spike proteins, etc.) (Artika et al., 2020), these viruses are expected to behave similarly in wastewater. Therefore, understanding how the surrogates behave compared to SARS-CoV-2 is integral to their utility in COVID-19 wastewater surveillance programs.

To account for sewershed variability, SARS-CoV-2 trends may be normalized by an endogenous reference. The pepper mild mottled virus (PMMoV) is an enteric virus that is ubiquitous in wastewater

(Kitajima et al., 2018) that has been commonly used as a means to normalize the SARS-CoV-2 surveillance data for fecal load in wastewater (Aguiar-Oliveira et al., 2020; Chik et al., 2021; D'Aoust et al., 2021; Wu et al., 2020). In some cases, normalizing against PMMoV has improved the SARS-CoV-2 trends over time (D'Aoust et al., 2021). However, normalizing against PMMoV may also worsen correlations between the SARS-CoV-2 signal and clinical cases (Ai et al., 2021; Dhiyebi et al., 2023b; Feng et al., 2021). Thus, understanding the partitioning behaviour of PMMoV compared to SARS-CoV-2 and the surrogates is also integral to the interpretation of said surveillance data.

The objective of this study is to contrast the partitioning of SARS-CoV-2, PMMoV, and two seeded surrogates (229E, MHV) in municipal wastewater samples. To examine viral partitioning, the RNA of these viruses in wastewater was concentrated through a series of experiments that target the separation of the liquid and solid fractions of wastewater (e.g., ultrafiltration, centrifugation). The goal of this study is to better understand the partitioning behaviour of SARS-COV-2, PMMoV, and potential surrogates (229E, MHV) in wastewater so that methods can be improved and inform the interpretation of wastewater surveillance data. The results were obtained during the COVID-19 pandemic using samples collected at several sites in Ontario, Canada.

2.2 Materials and Methods

Collected wastewater underwent a series of experiments that targeted the viral concentration step of the sample processing workflow (Figure 1). In brief, the collected wastewater was concentrated using centrifugation, ultrafiltration, and overnight PEG precipitation followed by centrifugation, then extracted for viral RNA, and finally quantified using reverse transcription qPCR. The first set of experiments (1-3) focused on the partitioning behaviour of the selected viruses (SARS-CoV-2, PMMoV, 229E, MHV) under five concentration conditions as described in section "2.2.2.1 Viral Partitioning (Experiments 1-3)." Experiment 4 compared the total RNA in the supernatant (liquid) using three ultrafiltration devices as described in section "2.2.2.2 Ultrafiltration Device Comparison (Experiment 4)." Conducting the research in real-time during the pandemic meant that experiments were dictated in part by material availability (e.g., ultrafiltration devices) and as RNA loads of SARS-CoV-2 in wastewater permitted (Figure A2).

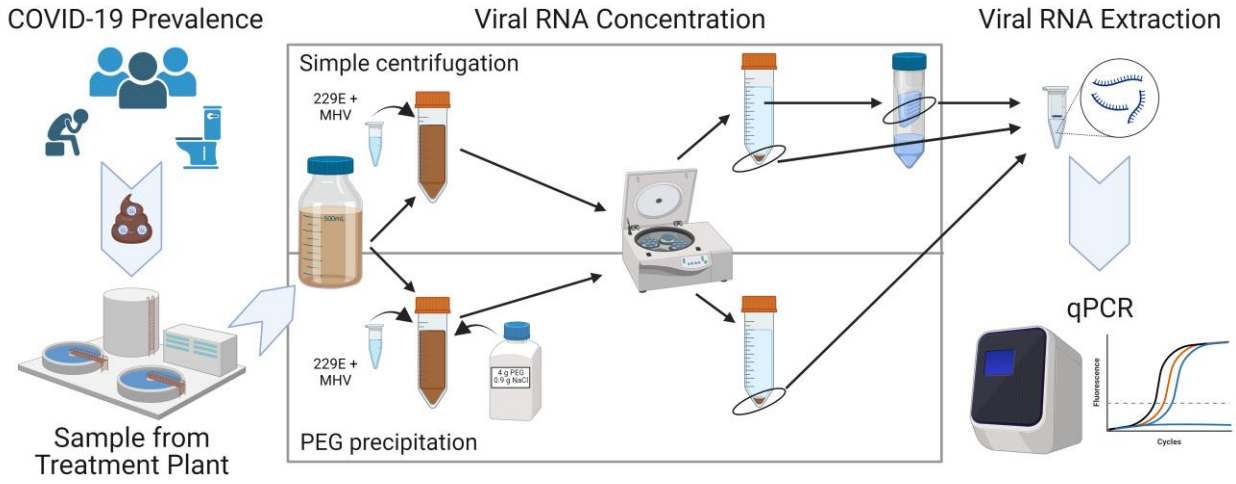

Figure 1. General workflow for wastewater sample processing. The viral RNA partitioning behaviour of SARS-CoV-2, PMMoV, 229E, and MHV was investigated by using liquid- and solid-based approaches during the concentration step as generally shown within the grey box. Figure created with BioRender.com.

2.2.1 Sample Collection

Wastewater (raw influent) was collected by plant operators from three municipal wastewater treatment plants (WWTP) located in southern Ontario, Canada. Based on 2021 estimates, the Clarkson (Region of Peel) WWTP services approximately 643,000 people with an average daily flow rate of 206 M litres per day (ML/d), the GE Booth (Region of Peel) WWTP services approximately 1.1 M people with an average daily flow rate of 434 ML/d, and Kitchener (Region of Waterloo) WWTP services approximately 256,000 people with an average daily flow rate of 66 ML/d (MECP, 2022). Wastewater was collected in pre-cleaned 250 mL HDPE bottles (Systems Plus, Baden, ON, Canada) from a 24-h chilled (4°C) composite sampler and shipped to the Servos Lab at the University of Waterloo via courier the same day in a small sterilized hard-shell cooler with ice or pre-frozen icepacks. On arrival, the sample bottles were wiped with 10% (v/v) bleach, rinsed with 70% (v/v) ethanol in a fume hood, then placed in a biosafety cabinet where they are exposed to ultraviolet light for 30 min before commencing the analysis. Following UV treatment, samples were placed in a fridge at 4°C with experiments commencing within 3 days (median timeframe) following collection (Table 1).

Table 1. Collection and extraction dates for the wastewater used for the experiments in this study.

Experiment	Contributing Proportion[a]	Collection Date	Extraction Date	Dominant SARS-CoV-2 Strain[b]	Reported Case Count[c]
Experiment 1A	33% Clarkson 67% GE Booth	Apr. 21, 2021	Apr. 22, 2021	Alpha	4359 8502
Experiment 1B	50% Clarkson 50% GE Booth	May 7, 2021	May 10, 2021	Alpha	3352 6783
Experiment 2	50% GE Booth 25% Clarkson 25% GE Booth	Sep. 21, 2021 Sep. 22, 2021 Sep. 22, 2021	Sep. 25, 2021	Delta	886 396 865
Experiment 3	[d]10% Clarkson [d]90% Clarkson	Jan. 19, 2022 Jan. 27, 2022	Jan. 29, 2022	Omicron	5717 3058
Experiment 4A	100% Kitchener	Dec. 30, 2021	Jan. 8, 2022	Omicron	2597
Experiment 4B	100% Clarkson	Jan. 19, 2022	Jan. 22, 2022	Omicron	5717

[a] Proportion of wastewater that was pooled for subsequent sample analysis.
[b] Dominant SARS-CoV-2 strain during the collection period was based on proportion throughout Ontario, Canada (Public Health Ontario, 2022).
[c] COVID-19 cases are by episode date as a rolling sum of the previous 14 days and are listed for each treatment plant based on the collection date. The data for the reported cases were extracted on December 14, 2022, from the Ontario Wastewater Surveillance Data and Visualization Hub which was developed by the Ministry of the Environment, Conservation and Parks (MECP) under the WSI (MECP 2022).
[d] Estimated proportions.

2.2.2 Testing Concentration Methods

Wastewater from the 250 mL collection bottles was pooled and following five inversions, 40 mL was randomly aliquoted into a sterile 50 mL conical tube that was placed immediately on ice. The 40 mL samples were then seeded with an estimate of 4.83-6.12 $\log_{10}$ copies of 229E virus and 4.57-5.33 $\log_{10}$ copies of MHV virus (Table A2; see Appendix B for culturing details), inverted five times and incubated for 10 min on ice. Following the incubation, samples were randomly selected for each treatment group (described below).

2.2.2.1 Viral Partitioning (Experiments 1-3)

The viral partitioning of RNA for SARS-CoV-2, PMMoV, 229E, and MHV in wastewater was conducted using a centrifugation-based approach. The use of centrifugation to measure the partitioning of viral RNA has the advantage of separating the wastewater into the liquid (supernatant) and solid (pellet) phases. With that in mind, the previously mentioned 40 mL wastewater aliquots were split randomly into five treatment groups. These treatment groups compared viral concentration methods (i.e., liquid- vs solid-based) and centrifugal force (Figure 2). The first set of tubes were centrifuged at 4,000 x *g* for 10 min with a brake (Condition A) with the supernatant (liquid) and pellets (solids) quantified as described below. The second set was centrifuged at 12,000 x *g* for 1.5 h with no brake (Condition B) with the supernatant (liquid) and pellets (solids) quantified. The final set of tubes underwent PEG precipitation (Condition C) followed by centrifugation at 12,000 x *g* for 1.5 h without a brake and the pellets (solids + liquid) quantified. Condition A (4,000 x *g*, 10 min, with brake) was based on methods reported in the literature for SARS-CoV-2 RNA wastewater analyses tailored for liquid-based (supernatant/ultrafiltration) protocols (Ahmed et al., 2020; Canadian Water Network, 2020; Torii et al., 2021). The other conditions were selected to be similar to the routine PEG precipitation protocol used for wastewater surveillance by the Servos Lab (Dhiyebi et al., 2023a) which was partially adapted from Wu et al. (2020).

Following surrogate incubation, supernatant and pellet treatments under Condition A (4,000 x *g*, 10 min, with brake) and Condition B (12,000 x *g*, 1.5 h, no brake) proceeded to centrifugation on the same day under their respective conditions. After centrifugation, the resulting supernatant was processed with a 10 kDa ultrafiltration device. Four replicates of the experiments were conducted using different ultrafiltration devices (partly based on availability during the pandemic) to process the supernatant fractions. Experiments 1A (Apr. 2021) and 1B (May 2021) were conducted with an Amicon Ultra-4 device (Millipore Sigma, Oakville, ON, Canada), Experiment 2 (Sep. 2021) was conducted with the Amicon Ultra-15 device (Millipore Sigma), and finally, Experiment 3 (Jan. 2022) was conducted using the Centricon Plus-70 device (Millipore Sigma). For each experiment, all manufacturer guidelines for the ultrafiltration devices were followed to concentrate the supernatant. In brief, the supernatant was loaded into the ultrafiltration device, centrifuged at 4,000 x *g* for the Amicon Ultra-4 (4 mL processed) and Amicon Ultra-15 (15 mL processed) devices and 3,500 x *g* for the Centricon Plus-70 device (40 mL processed). A maximum of 250 µL of the resulting concentrate was used for viral RNA extraction (as described below). The viral RNA signal in the supernatant fraction for SARS-CoV-2 for both Condition

A (4,000 x *g*, 10 min, with brake) and Condition B (12,000 x *g*, 1.5 h, no brake) during Experiment 2 was outside the dynamic range of the standard curve (1,000 to 1.6 copies/5 µL template) and was deemed below the method's ability to accurately quantify it. Therefore, only the pellet (solid) fraction and PEG precipitation/centrifugation data were analyzed. For all experiments, once the supernatant was transferred to the ultrafiltration device, the remainder was removed (poured without disturbing the pellet on the bottom) and the solid samples were centrifuged again for another 5 min (no brake) to solidify the pellet. The remaining supernatant was removed using a pipette and the pellet was weighed to three decimal places. If additional centrifugation was required due to pellet sluffing, samples were centrifuged again for 5 min with a moderate brake. A maximum weight of 250 mg of the pellet was taken for viral RNA extraction without further treatment (as described below).

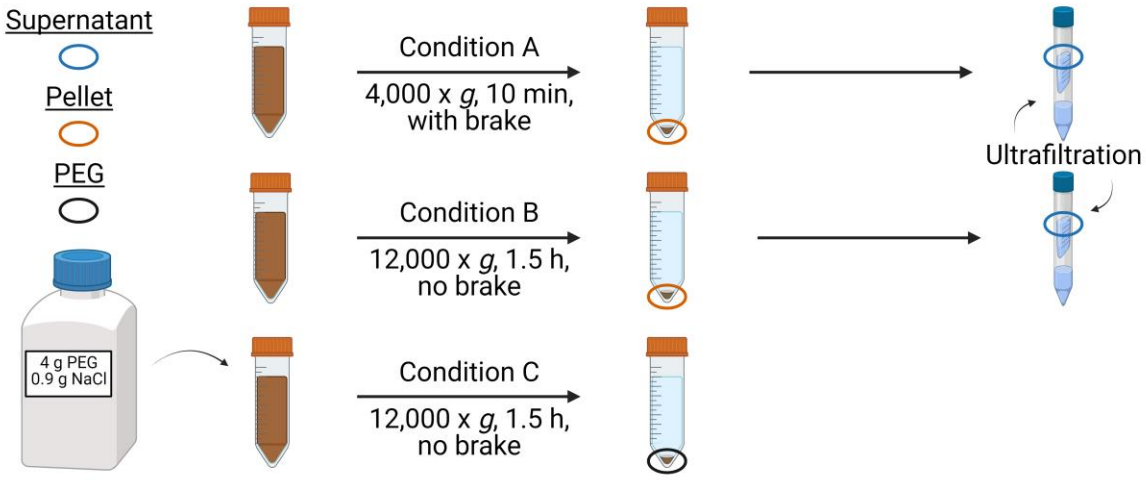

Figure 2. Overview of the approach to testing viral RNA partitioning behaviour (Experiments 1-3). Experiments 1A/B used an Amicon Ultra-4 device, Experiment 2 used an Amicon Ultra-15 device, and Experiment 3 used a Centricon Plus-70 device. Figure created with BioRender.com.

For PEG precipitation/centrifugation, following surrogate incubation, the 40 mL sample aliquots were transferred to a second set of 50 mL conical tubes containing 4 g (± 5%) PEG 8000 and 0.9 g (± 5%) NaCl (Fisher Scientific, Mississauga, ON, Canada). Next, they were shaken moderately for 5 sec, vortexed at 2,000 rpm for 30 sec (Digital Vortex Mixer, Fisher Scientific), and then placed on an Advanced 3500 Orbital Shaker (VWR, Mississauga, ON, Canada) for 2 h at 150 rpm inside a 4°C fridge

and then incubated overnight (15-18 h). After overnight incubation, samples were centrifuged at 12,000 x *g* for 1.5 h with no brake. The supernatant was removed and re-centrifuged for 5 min at 12,000 x *g* without a brake. A maximum of 250 mg of the pellet (i.e., a sub-sample for larger pellets) was taken for viral RNA extraction (as described below).

2.2.2.2 Ultrafiltration Device Comparison (Experiment 4)

Since three different ultrafiltration devices were used in the viral partitioning experiments (Experiments 1-3), it was important to directly compare these devices against each other. For this reason, the Amicon Ultra-4, Amicon Ultra-15, and Centricon Plus-70 devices were tested against each other in a head-to-head experiment (Experiment 4; Figure 3). Similar to Experiments 1-3, 40 mL of wastewater was randomly aliquoted across 50 mL conical tubes. However, only one centrifugal condition was used in Experiment 4 (12,000 x *g*, 1.5 h, no brake) to form the supernatant (liquid) and pellets (solids). While the focus of Experiment 4 was to compare the ultrafiltration devices that concentrate the viral RNA from the supernatant (liquid), the pellets (solids) were also processed for RNA extraction (Figure A3). In total, this head-to-head comparison was replicated twice in January 2022. Both the Amicon Ultra-4 and Ultra-15 devices used the same wastewater sample tube for the liquid fraction determination (i.e., one sample tube yielded two liquid fraction estimates for each of the Amicon devices). For the Centricon Plus-70 devices, 40 mL of supernatant was pipetted from a sample tube and loaded into the ultrafiltration device. All manufacturer guidelines were followed to concentrate the supernatant and a maximum of 250 µL of the concentrate was taken for viral RNA extraction.

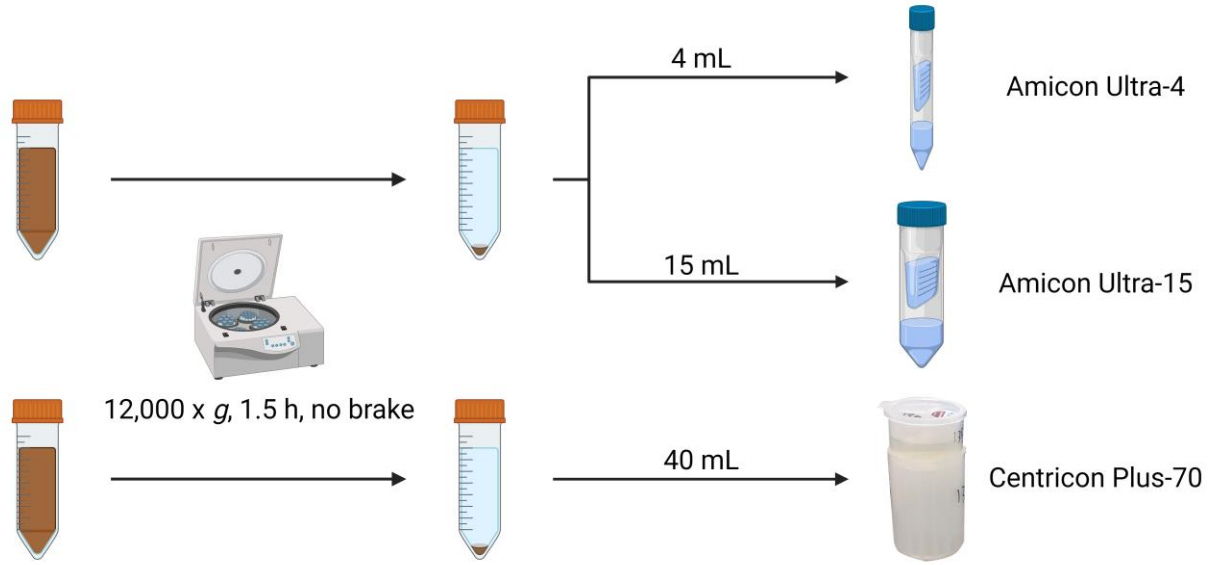

Figure 3. Overview of the approach for the ultrafiltration device comparison (Experiment 4). Figure created with BioRender.com.

2.2.3 Viral RNA Extraction

Viral RNA was extracted from the pellet and supernatant concentrates following manufacturer instructions using the RNeasy PowerMicrobiome Kit (Qiagen, Germantown, MD, USA) on a QIAcube Connect instrument (Qiagen) and eluted to 100 µL in RNase-free water. A protocol modification took place to the PM1 buffer and 2-mercaptoethanol addition step by adding 100 µL of TRIzol (Fisher Scientific) to promote cell lysis before bead-beating the sample. For Experiments 1A/B, a Vortex-Genie 2 (Scientific Industries, Bohemia, New York, USA) was used for 10 min set to maximum speed (3,000 rpm) to bead-beat the samples. For Experiments 2-4, a Bead Mill 24 Homogenizer (Fisher Scientific) was used for 5 min at 3.55 m/s to bead-beat the samples. This comparison indicated that both protocols yielded comparable viral RNA for all gene targets (unpublished data).

2.2.4 RT-qPCR

RNA extracts were quantified in triplicate by reverse transcription qPCR (qPCR) for two regions of the nucleocapsid (N) gene for endogenous SARS-CoV-2 (N1 and N2) using TaqPath™ 1-Step RT-qPCR Master Mix, CG (Life Technologies, Thermo Scientific, Burlington, ON, Canada) on the CFX96 Touch

or CFX Opus Real-Time PCR systems (Bio-Rad Laboratories, Hercules, CA, USA). Additionally, a region of the coat protein gene for endogenous PMMoV, a region of the membrane protein gene for exogenous (seeded) 229E, and a region of the N gene for exogenous (seeded) MHV was quantified using the same master mix and qPCR instrument (primer and probe sequences are presented in Table 2 and cycling conditions in Table 3). SARS-CoV-2 RNA was quantified with an RNA Exact Diagnostics (EDX) SARS-CoV-2 standard (Bio-Rad Laboratories) whereas all other targets were quantified using a dsDNA gBlock standard (Integrated DNA Technologies, Coralville, IA, USA) (Table 4) with all standards verified by dPCR (QIAcuity, Qiagen, Hilden, Germany). All plates were processed with positive controls (a standard with a known RNA concentration), non-template controls (all PCR reagents without a template), and non-reverse transcriptase controls (all PCR reagents without reverse transcriptase). Both N-gene targets and PMMoV were quantified using a simplex assay. The N-gene assay was performed in a 20 µL reaction with 5 µL of RNA template and the PMMoV assay was performed in a 10 µL reaction with 2.5 µL RNA template. The surrogates 229E and MHV were quantified in a duplex assay performed in a 10 µL reaction with 2.5 µL RNA template.

Finally, inhibition of reverse transcriptase and DNA polymerase was assessed with a master mix seeded with bacteriophage MS2 RNA (Millipore Sigma) and zebrafish (*Danio rerio*) DNA respectively (gBlock, IDT). Sample extracts were plated in duplicate and assessed for a one Cq shift compared to the positive control (sample replaced with RNase-free water) to indicate qPCR inhibition (Cao et al., 2012; Swango et al., 2006). With this method, there was no indication of qPCR inhibition for the samples.

Table 2. List of primers and probes used in this study that were supplied by Millipore Sigma.

Primer/Probe	Final Concentration (nM)	Sequence (5' to 3')	Probe Reporter/ Quencher	Reference
N1_FP	500	GACCCCAAAATCAGCGAAAT		(CDC, 2020)
N1_RP	500	TCTGGTTACTGCCAGTTGAATCTG		
N1_P	125	ACCCCGCATTACGTTTGGTGGACC	6-FAM / BHQ-1	
N2_FP	500	TTACAAACATTGGCCGCAAA		
N2_RP	500	GCGCGACATTCCGAAGAA		
N2_P	125	ACAATTTGCCCCCAGCGCTTCAG	6-FAM / BHQ-1	
PMMoV_FP	400	GAGTGGTTTGACCTTAACGTTGA		(Zhang et al., 2006)
PMMoV_RP	400	TTGTCGGTTGCAATGCAAGT		
PMMoV_P	125	CCTACCGAAGCAAATG	Cy5 / BHQ-1	
229E_FP	400	TTCCGACGTGCTCGAACTTT		(Vijgen et al., 2005)
229E_RP	400	CCAACACGGTTGTGACAGTGA		
229E_P	200	TCCTGAGGTCAATGCA	6-FAM / BHQ-1	
MHV_FP	300	GCCTCGCCAAAAGAGGACT		(Raaben et al., 2007)
MHV_RP	300	GGGCCTCTCTTTCCAAAACAC		
MHV_P	125	CAAACAAGCAGTGCCCAGTGCAGC	HEX / BHQ-1	
MS2_FP	900	TGCTCGCGGATACCCG		(Dreier et al., 2005)
MS2_RP	900	AACTTGCGTTCTCGAGCGAT		
MS2_P	250	ACCTCGGGTTTCCGTCTTGCTCGT	HEX / BHQ-1	
Zebrafish_FP	900	TGCGAAAAACACACCCAG		(Servos Lab, in house)
Zebrafish_RP	900	GGCAGATGAAGAAGAAGGAAG		
Zebrafish_P	250	CAATACACTACACCTCAGACATCTCAA CAGCA	6-FAM / BHQ-1	

Primer/Probe: FP = forward primer; RP = reverse primer; P = probe.

Table 3. Cycling conditions for qPCR reactions. The denature and anneal/elongation steps were repeated for 45 cycles.

Assay	Preheat (°C; min)	Reverse Transcription (°C; min)	Activation (°C; min)	Denature (°C; sec)	Anneal/ Elongation (°C; min)
N1 simplex	25; 2	50; 15	95; 2	95; 3	55; 30
N2 simplex	25; 2	50; 15	95; 2	95; 3	60; 30
PMMoV simplex	25; 2	50; 15	95; 2	95; 3	60; 30
229E+MHV duplex	25; 2	50; 15	95; 2	95; 3	60; 30
MS2+zebrafish duplex	25; 2	50; 15	95; 2	95; 3	60; 30

Table 4. List of synthetic oligonucleotides (gBlocks) sequences used in this study that were supplied by Integrated DNA Technologies.

Target	Sequence (5' to 3')
229E	GATGTACTTCGCAAACAGTTTCAGACTTTTCCGACGTGCTCGAACTTTTTGGGCAT GGAATCCTGAGGTCAATGCAATCACTGTCACAACCGTGTTGGGACAGACATACTA TCAACCCATTCAAC
MHV	TAACGAAGCAAAGTGCCAAAGAAGTCAGGCAGAAAATATTAAACAAGCCTCGCC AAAAGAGGACTCCAAACAAGCAGTGCCCAGTGCAGCAGTGTTTTGGAAAGAGAG GCCCCAATCAGAATTTTGGAGGCTCTGAAATGTTAAAACTTGGAACTAGTGATCCA CAGTTCCCCATTCTTGCAGAGTTGGCTCCAACAGTTGGTGCCTTCT
PMMoV	AGGTAATGGTAGCTGTGGTTTCAAATGAGAGTGGTTTGACCTTAACGTTTGAGAGG CCTACCGAAGCAAATGTCGCACTTGCATTGCAACCGACAATTACATCAAAGGAGG AAGGTTCGTTGAAG
Zebrafish (*Danio rerio*)	ATGACAAGCCTGCGAAAAACACACCCAGTTTTAAAAATCGCTAATGACGCATTAG TTGATTTGCCAACGCCACTAAATATTTCAGCGTGATGAAATTTTGGATCTCTCCTTG GATTATGTCTTATTACACAAATTTTAACAGGACTATTTTTAGCAATACACTACACCT CAGACATCTCAACAGCATTTTCATCTGTTGTGCATATTTGCCGAGATGTAAATTTC GGCTGACTTATTCGGAGCATCCATGCCAATGGGGCTTCCTTCTTCTTCATCTGCCTG TATATTCACATCGCCC

2.2.5 Data Analysis

An eight-point standard curve was used to quantify the samples (copies/well) for N1 and N2 whereas PMMoV, 229E, and MHV used a six-point standard curve. The supernatant (liquid) (Equation 1) and

pellet (solid) (Equation 2) fractions were then corrected for the elution volume and wastewater sample volume, as well as for pellet and liquid sub-sampling as applicable.

$$\textbf{Supernatant}_{\left(\frac{\textbf{copies}}{\textbf{40 mL}}\right)} = \frac{\textbf{cp}}{\textbf{well}} * \frac{\textbf{well}}{\textbf{template vol } (\mu\textbf{L})} * \textbf{elution vol } (\mu\textbf{L}) * \frac{\textbf{total vol (mL)}}{\textbf{ultrafiltration vol (mL)}} * \frac{\textbf{total conc vol } (\mu\textbf{L})}{\textbf{extracted conc vol } (\mu\textbf{L})} * \frac{\textbf{1}}{\textbf{40 mL}} \quad (1)$$

$$\textbf{Pellet}_{\left(\frac{\textbf{copies}}{\textbf{40 mL}}\right)} = \frac{\textbf{cp}}{\textbf{well}} * \frac{\textbf{well}}{\textbf{template vol } (\mu\textbf{L})} * \textbf{elution vol } (\mu\textbf{L}) * \frac{\textbf{total pellet mass (g)}}{\textbf{extracted pellet mass (g)}} * \frac{\textbf{1}}{\textbf{40 mL}} \quad (2)$$

A one-way ANOVA was used to test if the concentration methods yielded the same log-transformed copies per 40 mL of wastewater across centrifugal conditions. In addition, a one-way ANOVA was also conducted to test for the disparity between ultrafiltration methods once corrected to log-transformed copies per 40 mL of wastewater. Following a significant ANOVA test, pairwise comparisons were made using Tukey's post-hoc test. All assumptions were reviewed including the assumption of normality (Shapiro-Wilk test and Q-Q plot) as well as the assumption of homoscedasticity (Levene's test). Finally, all statistical tests implemented a p-value threshold of 0.05 and were conducted using R version 4.0.5 (R Core Team, 2021).

2.3 Results

2.3.1 Viral Partitioning

The RNA copies of the study targets (N1, N2, PMMoV, 229E, MHV) were compared in a series of experiments that examined their partitioning behaviour in wastewater. Across the four experiments, the tested treatments with different concentration methods (centrifugation, ultrafiltration, overnight PEG precipitation followed by centrifugation) and centrifugal conditions (4,000 x *g*, 10 min, with brake and 12,000 x *g*, 1.5 h, no brake) showed a high degree of reproducibility in the observed partitioning patterns for each target (Figure 4-6). In addition, the comparison of RNA copies between treatments (concentration method with the centrifugal condition) for all targets showed significant differences for the one-way ANOVA test ($p < 0.017$; full results are available in Appendix C: Table C1). When excluding Experiment 2 (further explained below), a substantial proportion of N1 (59-78%), N2 (66-83%), 229E (81-97%), and MHV (61-92%) were observed in the supernatant fractions under Condition A (4,000 x *g*,

10 min, with brake). Under Condition B (12,000 x *g*, 1.5 h, no brake), these targets show near equal partitioning between the supernatant (liquid) and pellet (solid) fraction for Experiments 1A/B and 3. Regardless of the condition, PMMoV remained primarily in the supernatant fraction (>78%). Overnight PEG precipitation followed by centrifugation had improved recovery for all targets over pellets (solids) alone by over 3-fold across Experiments 1-3.

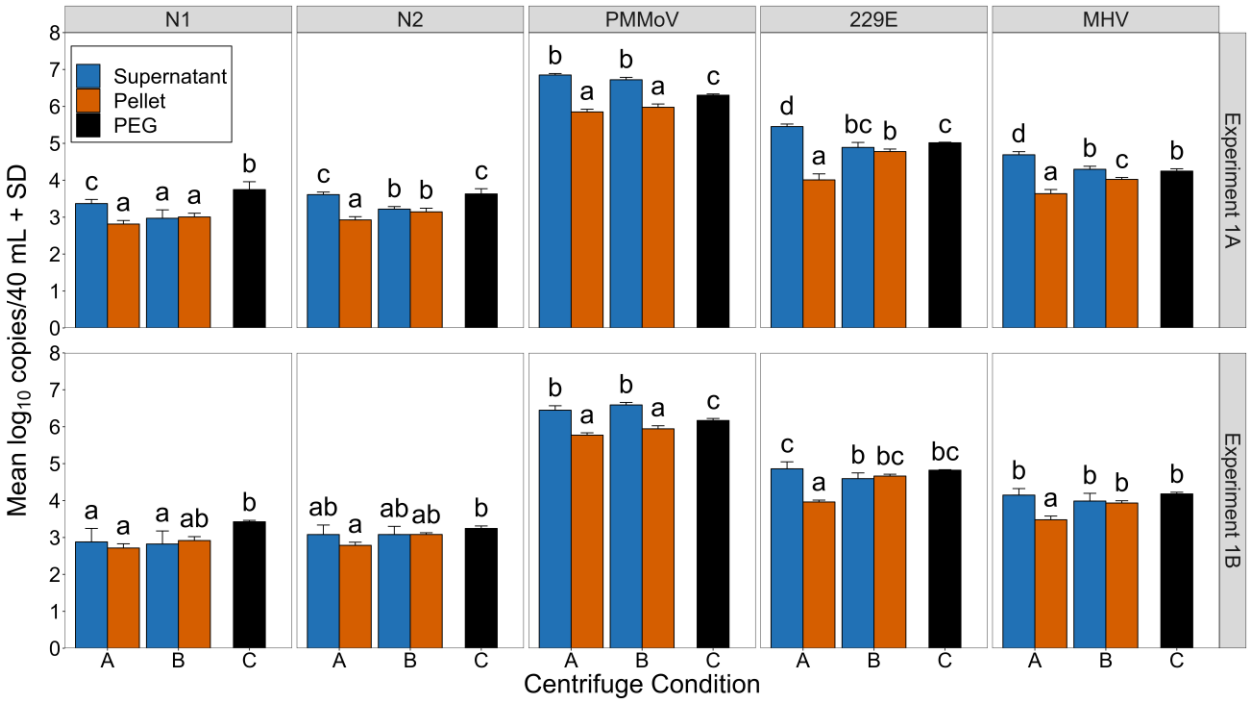

Figure 4. Experiments 1A/B: Effect of centrifugal condition measured by RNA copies per 40 mL of wastewater for SARS-CoV-2 (N1 and N2), PMMoV, 229E, and MHV. All treatments were n = 4 and the supernatant fraction was processed through an Amicon Ultra-4 device using 4 mL of wastewater for both experiments.

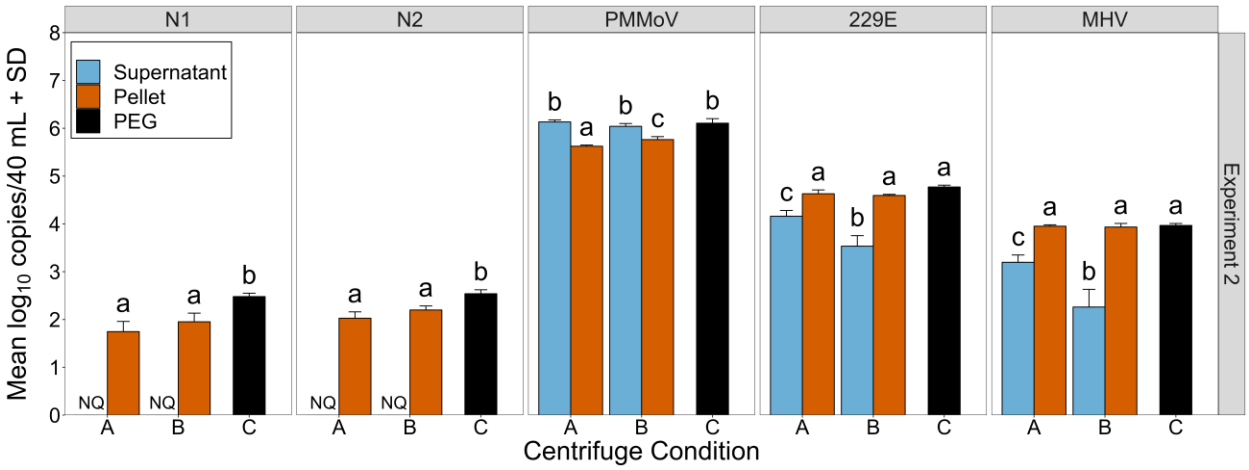

Figure 5. Experiment 2: Effect of centrifugal condition measured by RNA copies per 40 mL of wastewater for SARS-CoV-2 (N1 and N2), PMMoV, 229E, and MHV. All treatments were n = 4 and the supernatant fraction was processed through an Amicon Ultra-15 device using 15 mL of wastewater. Note that NQ = non-quantifiable.

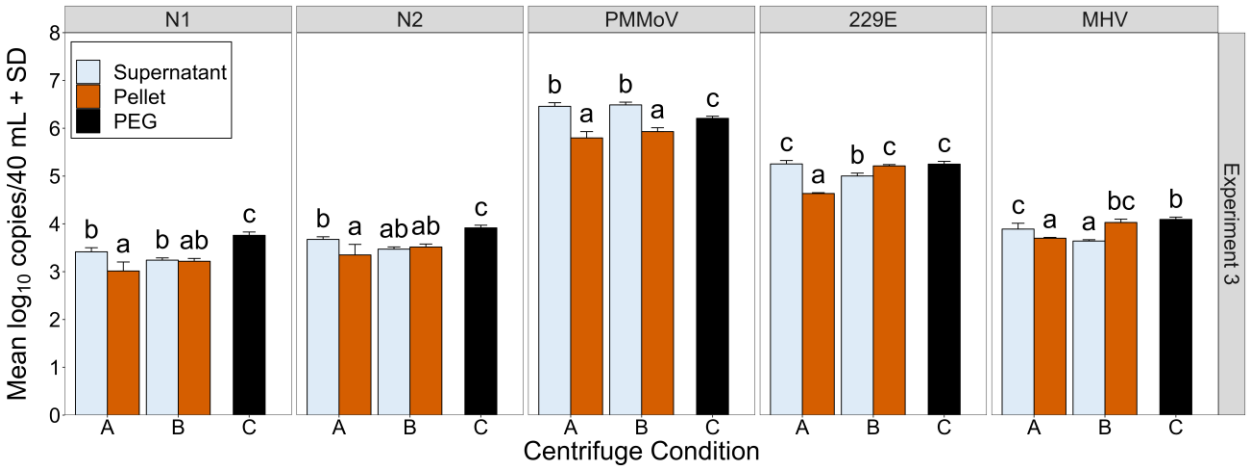

Figure 6. Experiment 3: Effect of centrifugal condition measured by RNA copies per 40 mL of wastewater for SARS-CoV-2 (N1 and N2), PMMoV, 229E, and MHV. All treatments were n = 4 and the supernatant fraction was processed through a Centricon Plus-70 device using 40 mL of wastewater.

The partitioning pattern of RNA copies for N1 and N2 were very similar across Experiments 1-3 (Figure 4-6). Between the supernatant (liquid) treatment processed by ultrafiltration and pellet (solid)

treatment for Condition A (4,000 x *g*, 10 min, with brake), the comparison of RNA copies for both N-gene targets in Experiment 1A (Figure 4) and Experiment 3 (Figure 6) showed significant Tukey pairwise differences ($p < 0.002$) but Experiment 1B (Figure 4) did not ($p > 0.127$). Furthermore, under Condition A (4,000 x *g*, 10 min, with brake), 59-83% of the N-gene RNA signal was captured by the supernatant (liquid) fraction across experiments when Experiment 2 is not included. In Experiment 2, an Amicon Ultra-15 device was used that showed 37-59% of the N-gene signal in the supernatant (liquid) under Condition A (4,000 x *g*, 10 min, with brake). When comparing the RNA copies in the supernatant (liquid) against the pellet (solid) under Condition B (12,000 x *g*, 1.5 h, no brake), Experiments 1A/B, and 3 were not significantly different ($p > 0.810$). For these experiments, the split of RNA copies between fractions ranged from 45-55%. The comparison of RNA copies of N1 and N2 between Condition A (4,000 x *g*, 10 min, with brake) and Condition B (12,000 x *g*, 1.5 h, no brake) for the same fraction generally saw non-significant Tukey differences except for three out of the 14 potential comparisons: N1 in Experiment 1A (Condition A supernatant to Condition B supernatant, $p = 0.023$); N2 in Experiment 1A (Condition A supernatant to Condition B supernatant, $p < 0.001$; and Condition A pellet to Condition B pellet, $p = 0.043$).

When the RNA copies of N1 and N2 were measured in the pellet (solid) fraction using Condition B (12,000 x *g*, 1.5 h, no brake) and were compared directly to the pellet obtained after PEG precipitation followed by centrifugation (12,000 x *g*, 1.5 h, no brake; Condition C), the PEG precipitation treatment was higher by a mean factor of 3.10 ± 1.12 SD across the four partitioning experiments (Figure A4-A6). More specifically, the target N1 was consistently higher by a mean factor of 3.90 ± 1.08 SD whereas N2 was consistently higher by a mean factor of 2.31 ± 0.67 SD across the four partitioning experiments. When SARS-CoV-2 RNA concentrations were the lowest during Experiment 2, the RNA copies of N1 for Condition C (PEG precipitation; 12,000 x *g*, 1.5 h, no brake) were 3.37-fold higher than the pellet from Condition B (12,000 x *g*, 1.5 h, no brake). Similarly, the RNA copies of N2 for Condition C (PEG precipitation; 12,000 x *g*, 1.5 h, no brake) were 2.19-fold higher than the pellet from Condition B (12,000 x *g*, 1.5 h, no brake).

The partitioning patterns of RNA copies for PMMoV were highly reproducible in this study except in Experiment 2. In Experiments 1A/B (Figure 4) and 3 (Figure 6), the RNA copies for the supernatant (liquid) treatments between Condition A (4,000 x *g*, 10 min, with brake) and Condition B (12,000 x *g*, 1.5 h, no brake) had non-significant Tukey pairwise comparisons ($0.075 < p < 0.985$). For the RNA copies of PMMoV for the pellet (solid) treatments between Condition A (4,000 x *g*, 10 min, with brake) and

Condition B (12,000 x *g*, 1.5 h, no brake), there were also non-significant Tukey differences ($0.060 < p < 0.220$). The RNA copies measured in the supernatant (liquid) for PMMoV ranged from 65-91% of the total signal in the sample. However, Experiment 2 had the lowest percentage of RNA copies for PMMoV in Condition A (4,000 x *g*, 10 min, with brake) at 76%. Additionally, for Condition B (12,000 x *g*, 1.5 h, no brake), 65% of the PMMoV copies were measured in the supernatant (liquid) fraction. Together, these two lower measurements during Experiment 2 added to the variability of PMMoV RNA measured in the supernatant (liquid).

Overnight PEG precipitation followed by centrifugation at 12,000 x *g* for 1.5 h without a brake (Condition C) had higher RNA copies of PMMoV than the pellet (solid) treatments alone but less than the RNA copies that were in the supernatant (liquid) treatments measured by the ultrafiltration devices (Figure 4-6). However, in Experiment 2 (Figure 5) both the supernatant (liquid) treatments and PEG precipitation were not significantly different ($p > 0.565$); differing from the other three experiments (1A/B, 3). Finally, the RNA copies from PEG precipitation (Condition C) were on average 1.97-fold ± 0.24 SD greater than the pellet (solid) treatment under the same centrifuge condition of 12,000 x *g* for 1.5 h without a brake (Figure A4-A6) across the four partitioning experiments.

The general partitioning patterns of the RNA copies for the surrogates 229E and MHV were similar across all experiments. However, there was variability with what centrifugal conditions were determined to be significantly different. For Experiments 1A/B (Figure 4) and 3 (Figure 6), the RNA copies for the surrogates under Condition A (4,000 x *g*, 10 min, with brake) were enriched in the supernatant (liquid) fraction. For 229E, the RNA copies in the supernatant (liquid) fraction ranged from 81-97% and for MHV the RNA copies in the supernatant (liquid) fraction ranged from 61-92%. The Tukey pairwise comparisons between the supernatant (liquid) and pellet (solid) treatments were significant for Experiments 1A/B and 3 ($p < 0.009$). In Experiment 2 (Figure 5), the RNA copies in the supernatant (liquid) treatment were lower than the RNA copies in the pellet (solid) treatment for both 229E ($p < 0.001$) and MHV ($p < 0.001$) and only comprised 25% and 15% of the sample total respectively.

PEG precipitation followed by centrifugation at 12,000 x *g* for 1.5 h without a brake (Condition C) had greater RNA copies for 229E and MHV than the pellet (solid) treatment under Condition B (12,000 x *g*, 1.5 h, no brake). Across the four experiments (1-3), there was an average factor of 1.44 ± 0.27 more RNA copies of 229E with PEG precipitation than the pellets (solids) processed without PEG precipitation under the shared centrifugal condition (Figure A4-A6). Similarly, for RNA copies of MHV, there was an

observed increase by a factor of 1.42 ± 0.35 when PEG precipitation was used than the pellet (solid) treatment under Condition B (12,000 x *g*, 1.5 h, no brake). Despite these average increases, only Experiment 1A (Figure 4) showed significant Tukey differences for the RNA copies between the pellet (solid) treatment under Condition B (12,000 x *g*, 1.5 h, no brake) and PEG precipitation (Condition C; 12,000 x *g*, 1.5 h, no brake) for both 229E ($p = 0.039$) and MHV ($p = 0.010$). Here, the observed increase by PEG precipitation (Condition C; 12,000 x *g*, 1.5 h, no brake) was 1.73-fold and 1.68-fold respectively.

2.3.2 Ultrafiltration Device Comparison

The RNA copies of the study targets (N1, N2, PMMoV, 229E, MHV) were compared using the Amicon Ultra-4, Amicon Ultra-15, and Centricon Plus-70 devices. Generally, there was a high degree of reproducibility between both experiments (4A/B) of the ultrafiltration device comparisons (Figure 7). The comparison of RNA copies between treatments (ultrafiltration devices) for all targets showed significant differences for the one-way ANOVA test ($p < 0.001$; full results are available in Appendix C: Table C2). There was a consistent observation across all targets that the Amicon Ultra-15 device had the lowest RNA copies and the Centricon Plus-70 device had the highest RNA copies during both experiments (4A/B). The three ultrafiltration devices selected for this study highlight a high degree of reproducibility but did not provide equivalent estimates. For all targets, the Amicon Ultra-4 device and the Centricon Plus-70 device quantified similar RNA copies, but the two devices were not equivalent. This pattern was observed in both ultrafiltration device comparisons (Experiment 4A/B; Figure 7).

The Amicon Ultra-15 and Centricon Plus-70 devices had similar RNA copies for N1 and N2 during both ultrafiltration device comparison experiments (4A/B; Figure 7). The RNA copies for N2 in Experiment 4A were the only comparison of the N-gene targets to have a non-significant pairwise comparison ($p = 0.450$) between the Amicon Ultra-4 and the Centricon Plus-70 devices. Accordingly, the RNA copies of N2 in Experiment 4B and N1 in both Experiments 4A/B were significantly different ($p < 0.033$). The difference between mean RNA copies for the Amicon Ultra-4 and Centricon Plus-70 devices for N1 in Experiment 4A was 0.20 log RNA copies ($p = 0.033$) versus 0.14 log RNA copies for N2 ($p = 0.450$). In Experiment 4B, the log difference between means was 0.49 copies ($p < 0.001$) and 0.27 copies ($p = 0.014$) for N1 and N2 respectively. The Amicon Ultra-15 device had the lowest measured concentrations for both N-gene comparisons ($p < 0.002$) compared to either the Amicon Ultra-4 or the Centricon Plus-70 devices.

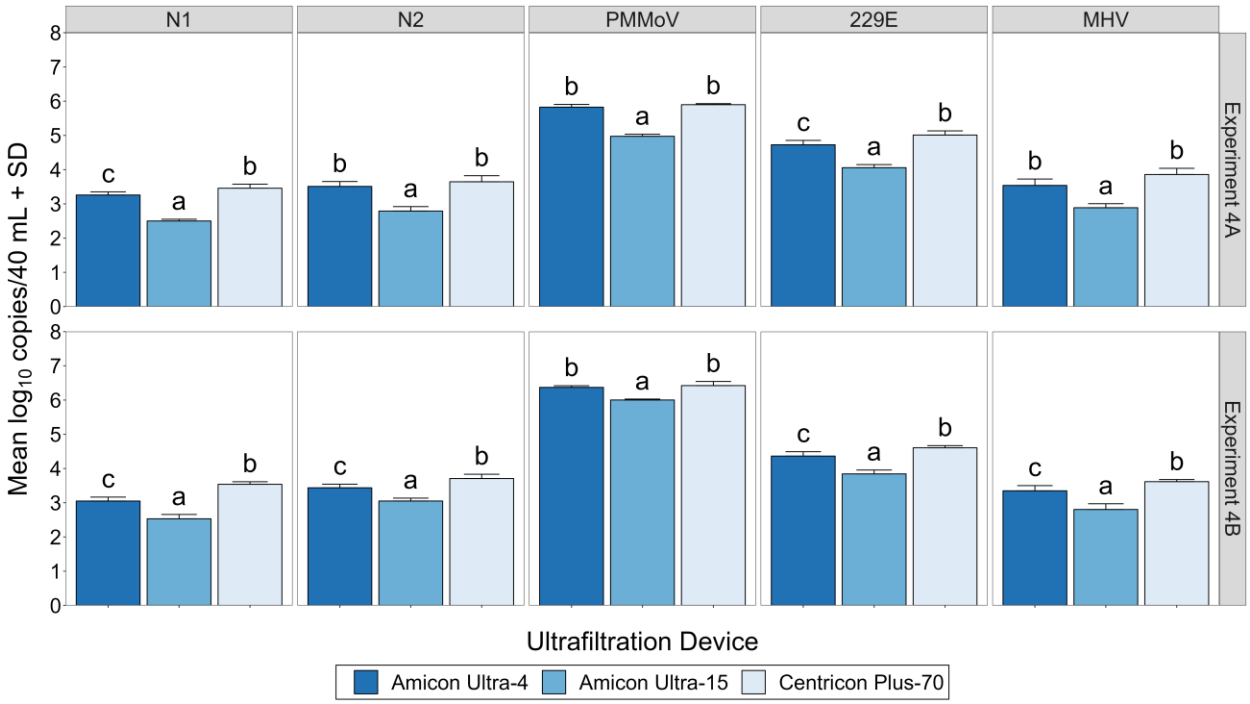

Figure 7. Experiment 4A/B: Comparison of three 10 kDa ultrafiltration devices measured by RNA copies per 40 mL of wastewater for SARS-CoV-2 (N1 and N2), PMMoV, 229E, and MHV. All treatments were n = 4.

The RNA copies for PMMoV had the same pattern for both replicates of the ultrafiltration device comparison (Experiment 4A/B; Figure 7). First, the RNA copies of PMMoV for the Amicon Ultra-4 and Centricon Plus-70 devices were not significantly different using Tukey's post-hoc test for Experiment 4A ($p = 0.265$) and Experiment 4B ($p = 0.620$). Additionally, the RNA copies of PMMoV for the Amicon Ultra-15 device were significantly different for Tukey's post-hoc comparison than both the Amicon Ultra-4 and Centricon Plus-70 devices ($p < 0.001$) for both Experiments 4A/B. Overall, copies of PMMoV measured by the three ultrafiltration devices were highly reproducible between Experiments 4A/B. Moreover, the Amicon Ultra-15 device consistently had lower RNA copies of PMMoV compared to the Amicon Ultra-4 and Centricon Plus-70 devices.

The partitioning patterns of RNA copies of the surrogates 229E and MHV were in line with the results observed by N1, N2, and PMMoV (Figure 7). Tukey's pairwise comparisons for 229E were significantly different for all combinations of ultrafiltration devices in Experiments 4A/B ($p < 0.024$). The RNA copies

of 229E for the Amicon Ultra-4 device were closer to the Centricon Plus-70 device in Experiment 4A ($p = 0.016$) and 4B ($p = 0.024$) than it was against its Amicon Ultra-15 device counterpart ($p < 0.001$) for both experiments (4A/B). Interestingly, the comparison for the RNA copies of MHV for the Amicon Ultra-4 and Centricon Plus-70 devices was close between Experiment 4A and 4B. In Experiment 4A, the comparison was not significantly different ($p = 0.054$) but in Experiment 4B it was ($p = 0.050$). Similar to 229E and the other targets (N1, N2, PMMoV), the Amicon Ultra-15 device gave consistently lower concentrations for MHV than both the Amicon Ultra-4 and Centricon Plus-70 devices in both experiments ($p < 0.001$).

2.4 Discussion

Understanding the apparent partitioning of viruses in wastewater is important to ensure a more informed interpretation of SARS-CoV-2 trends in wastewater. The apparent partitioning of SARS-CoV-2 (N1, N2) and PMMoV in wastewater were affected by modifications to the concentration step, including PEG precipitation, and the centrifugation speed applied. Increasing centrifugation speed from 4,000 x *g* (10 min, with brake) to 12,000 x *g* (1.5 h, no brake) increased the proportion of RNA for both N1 and N2 in the pellet (solid) fraction with the total amount splitting almost equally between the pellet (solid) and supernatant (liquid). Overnight PEG precipitation followed by centrifugation (12,000 x *g*, 1.5 h, no brake) increased the concentration of N1 and N2 recovered in the pellet fraction by about 310% of the RNA signal in the pellet without PEG precipitation. The Amicon Ultra-15 device was much less effective at concentrating the viruses than the other filtration devices (Amicon Ultra-4 and Centricon Plus-70). Both 229E and MHV added as surrogates followed a similar trend to the N1 and N2 but were less pronounced. The biomarker PMMoV which is often used to normalize the SARS-CoV-2 signal behaved distinctly different with it being primarily found in the supernatant (liquid) fraction even with PEG precipitation. Collectively the results of the current study suggest that when using centrifugation- or ultrafiltration-based approaches care must be taken to interpret SARS-CoV-2 WBS data. This is because centrifugal conditions and ultrafiltration apparatuses impact the apparent partitioning that can lead to differences in the recovery of the viruses in each phase.

2.4.1 Viral Partitioning

As N1 and N2 are sequences on the N-gene it is expected that they would provide equivalent results across the partitioning and ultrafiltration experiments. After centrifugation at only 4,000 x *g* for 10 min with a brake (Condition A), RNA copies of both N1 and N2 were found predominantly in the supernatant.

Interestingly, when the centrifugal condition was at 12,000 x *g* for 1.5 h without a brake (Condition B), RNA copies of N1 and N2 were distributed almost evenly. This confirmed that N1 and N2 gene targets responded in tandem with each other across the various experimental conditions and demonstrated that a substantial portion of SARS-CoV-2 RNA is left in the supernatant fraction following either centrifugal condition. Others have observed that N1 and N2 RNA concentrations respond to experimental conditions in a similar fashion with Kim et al. (2022) noting N1 and N2 were correlated with each other in both the liquid and solid fractions of wastewater. In like manner, RNA copies of both surrogates (229E, MHV) under Condition B (12,000 x *g*, 1.5 h, no brake) generally split evenly between the supernatant (liquid) and pellet (solid) fraction similar to SARS-CoV-2 (Figure 4, 6). Conversely, RNA copies 229E and MHV tended to partition further to the supernatant fraction under Condition A (4,000 x *g*, 10 min, with brake) than SARS-CoV-2 indicating that under this condition, the surrogates may behave differently. A similar observation was noted by Chik et al. (2021) in an interlaboratory study with the surrogate 229E showing a tendency to partition more to the liquid fraction than SARS-CoV-2. However, in their interlaboratory study, there were various methods used to separate the liquid and solid phases such as centrifugation (8,000 x *g*), filtration (22 µm or 45 µm), gravitational settling, or a combination of these. Accordingly, these methods may then have inherent differences in the way they determine apparent partitioning. In Experiment 2 (Figure 5), the Amicon Ultra-15 device was unable to detect SARS-CoV-2 RNA in the supernatant (liquid) fraction. However, both surrogates indicated a lower-than-expected recovery in the supernatant (liquid) fraction compared to previous experiments (1A/B). This suggested that the poor recovery for SARS-CoV-2 was in part driven by the performance of the Amicon Ultra-15 device as well as it being a period where clinical cases and SARS-CoV-2 RNA concentrations in wastewater were already low (Table 1; Figure 5). Overall, the apparent partitioning of the RNA for SARS-CoV-2 (N1, N2) and the surrogates (229E, MHV) is not constant but rather a reflection of the concentration method that was used.

The addition of overnight PEG precipitation (Condition C, 12,000 x *g*, 1.5 h, no brake) increased the concentration detected in the pellet by 3.10-fold relative to the similar condition without PEG precipitation (Condition B; Figure A4-A6). It is possible to increase the yield of SARS-CoV-2 RNA in a pellet fraction by increasing the centrifugation as previously discussed as well as through the addition of overnight PEG precipitation followed by centrifugation. Although a few studies have compared the direct capture of the solids with PEG precipitation (LaTurner et al., 2021; Pecson et al., 2021) they did not use the same conditions as this study. Most often, the solids are first removed from the wastewater sample

using filtration or centrifugation prior to PEG precipitation. As a result, the PEG precipitation method may have lower RNA concentrations than a solids-only method (LaTurner et al., 2021; Pecson et al., 2021) but the approaches are not directly comparable. In our study, under the same condition (12,000 x *g*, 1.5 h, no brake), it is evident that PEG precipitation without removing the solids improves the overall SARS-CoV-2 RNA recovery.

Contrary to SARS-CoV-2 (i.e., N1, N2), PMMoV had a different pattern across the partitioning experiments. The centrifugal condition had a minimal or no effect on the recovery of the virus in each phase. Regardless of the condition, RNA copies of PMMoV remained primarily in the supernatant fraction (65-91%). Although PEG precipitation increased the RNA copies of PMMoV measured in the pellet (1.97-fold), the majority of PMMoV remained in the supernatant (as recovered by ultrafiltration devices). Since PMMoV is ubiquitous in wastewater (Kitajima et al., 2018), it has been widely used to normalize the SARS-CoV-2 signal to improve trends over time by accounting for the apparent variability in fecal content of the samples (D'Aoust et al., 2021; Wu et al., 2020). However, the apparent partitioning differences from SARS-CoV-2 do raise further questions about its application as an endogenous reference to normalize against. It has also been shown that PMMoV RNA can persist in wastewater longer than SARS-CoV-2 RNA at varying temperatures (4°C, 12°C, 20°C) with this observation exacerbated in the liquid (solids removed) fraction (Burnet et al., 2023). Therefore, it is possible that under some conditions, normalizing the SARS-CoV-2 wastewater signal with PMMoV may result in additional variability (Burnet et al., 2023). Moreover, the differences in the apparent partitioning of PMMoV in the liquid fraction compared to SARS-CoV-2 may also lead to additional variability as the fate of the two viruses may differ. Another aspect to consider is that ultrafiltration devices may co-concentrate inhibitors that exist in the liquid fraction (Ahmed et al., 2020) and this could alter estimated concentrations of either virus. Moreover, inhibition of qPCR is also an important consideration in the pellets (solids) obtained by centrifugation. Inhibition is often addressed by dilution (Wilson, 1997) but at low SARS-CoV-2 RNA concentrations, this may not be an option. Regardless, there is additional complexity to consider when the partitioning of the target of interest differs from what it is being normalized against. While many studies have examined alternative biomarkers for normalization such as cross-assembly phage (crAssphage) (Ai et al., 2021), human *Bacteroides* HF183 (Feng et al., 2021), or various chemical compounds such as caffeine or paraxanthine (Hsu et al., 2022), none will truly mimic SARS-CoV-2 in wastewater. Be it as it may, PMMoV remains the popular choice which could be attributed to its early adoption in WBS programs. However, PMMoV normalization can lead to additional variability in trends (Dhiyebi et al.,

2023b; Feng et al., 2021) and its use in surveillance programs continues to be debated. Since the apparent partitioning of SARS-CoV-2 RNA and PMMoV RNA are not the same, caution should be used when interpreting normalized SARS-CoV-2 RNA trends as their fates may differ.

There is a general consensus that SARS-CoV-2 should partition to the solids due to its enveloped structure (Ahmed et al., 2020; Kitamura et al., 2021) as the lipid bilayer provides lipophilic characteristics (Schoeman & Fielding, 2019). Using two enveloped viruses, MHV and *Pseudomonas* phage ϕ6, and two non-enveloped viruses, *Enterobacteria* phage MS2 and T3, Ye et al. (2016) showed that seeded enveloped viruses adsorbed to the solid fraction in wastewater in greater proportion than the seeded nonenveloped viruses when the solids were removed from the wastewater using a centrifugal condition of 30,000 x *g* for 10 min. With this condition, a maximum of 26% of the enveloped viruses were determined to adsorb to the solid fraction while nonenveloped viruses were estimated to have a maximum of 6% adsorb to solids (Ye et al., 2016). However, the adoption of solid-based approaches fails to recognize that a major proportion of the viral signal may remain in the liquid phase of the wastewater. To add to these adsorption considerations, Wellings (1976) noted that viruses are part of the solid fraction through both adsorption and being integrally part of the solids (i.e., embedded) and that methods often fail to recognize the latter. With the virus embedded in feces, it has been suggested that this may act as a form of protection from degradation (Rahimi et al., 2021). This explains why samples can be held for many days without a major shift in the SARS-CoV-2 signal (Hokajärvi et al., 2021; Islam et al., 2022; Simpson et al., 2021).

As previously mentioned, there has been a strong emphasis in the literature on solid-based approaches for measuring SARS-CoV-2 RNA in wastewater (Chik et al., 2021; D'Aoust et al., 2021; Graham et al., 2021; Kim et al., 2022; Kitamura et al., 2021). Commonly, partitioning results are reported on a concentration basis (e.g., copies/mL or copies/g) that makes the solid fraction appear more important (Graham et al., 2021; Kim et al., 2022) even though the largest portion of the virus may remain in the liquid/colloidal phase (Table A3). Based on the total copies in each phase, it is evident that SARS-CoV-2 exists almost equally between the supernatant (liquid) and pellet (solid) fractions under Condition B (12,000 x *g*, 1.5 h, no brake). As the force and time are reduced to 4,000 x *g* for 10 min with a brake (Condition A), SARS-CoV-2 RNA exists primarily in the supernatant (59-83%, range excludes Experiment 2) instead of the even split under Condition B (12,000 x *g*, 1.5 h, no brake). To only target and quantify the solid fraction eliminates at least half of the RNA signal if conditions are similar to either Condition A (4,000 x *g*, 10 min, with brake) or Condition B (12,000 x *g*, 1.5 h, no brake). Therefore, this

study supports that although SARS-CoV-2 enriches in the solid fraction due to a substantially lower solids-to-liquid ratio in the wastewater, a large proportion (approximately 50-80%), remains in the supernatant fraction (depending on the conditions). It is likely that SARS-CoV-2 RNA is associated with very small particles or colloidal material that does not settle during centrifugation.

It is still unknown if the SARS-CoV-2 virus remains intact, fragmented, or degraded in wastewater by the time it reaches the concentration step in the quantification process (Graham et al., 2021; Hill et al., 2021; LaTurner et al., 2021). Based on correlative light fluorescence and electron microscopy, at least some intact SARS-CoV-2 virus may exist in wastewater (Belhaouari et al., 2021). Additionally, the intact virus may exist in wastewater but remain noninfective due to enzymatic modifications to the spike protein in the digestive tract before being shed into sewer systems (Robinson et al., 2022). It is unlikely that fully intact SARS-CoV-2 virus exists in wastewater, but the RNA may also be shielded by ribonucleoprotein complexes (Mondal et al., 2021) and therefore protected from rapid degradation in the wastewater. It is therefore likely that a combination of mostly intact and fragmented SARS-CoV-2 RNA exists in wastewater that is both adsorbed to and embedded within the solids.

Piecing the above together, there is an alignment between the results of this study and what has been described in the literature. First, large solids that are easily pelleted (Condition A; 4,000 x *g*, 10 min, with brake) would contain viral RNA embedded within as well as adsorbed to the outside. Secondly, the remaining viral RNA, to an extent, can be pelleted further (Condition B; 12,000 x *g*, 1.5 h, no brake) suggesting that the viral RNA is still embedded or adsorbed to finer material in some capacity. Moreover, chemical facilitation through PEG precipitation followed by centrifugation (Condition C) improves RNA recoverability through the reduction of solvent (i.e., H_2O) availability thereby promoting an environment for genetic material to be displaced and pelleted more readily (Atha & Ingham, 1981; Poison, 1977). Interestingly, PEG and NaCl can also degrade the lipid bilayer (Boni et al., 1981; Cordova et al., 2003). This potential modification to the structure of enveloped viruses in wastewater adds additional complexity to what exactly is being captured by the concentration methods. On one hand, some have noted PEG precipitation followed by centrifugation to be poor for enveloped viruses (Kitamura et al., 2021; Ye et al., 2016). However, the use of PEG and NaCl prior to centrifugation has also been successful at isolating SARS-CoV-2 (Barril et al., 2021). In the current study, PEG precipitation followed by centrifugation is improved over a non-PEG precipitation approach using the same centrifugal condition of 12,000 x *g* for 1.5 h without a brake where no initial solid removal took place (Figure A4-A6). Finally, it has been documented that DNA adsorbed to soil colloids and minerals was protected from degradation from

DNases (Cai et al., 2006). Therefore, it is plausible that RNA in the supernatant (liquid) phase is adsorbed to colloidal material and shielded from degradation in wastewater. Thus, the colloidal material is captured by the membrane of the ultrafiltration device along with SARS-CoV-2 RNA and other viruses that may be adsorbed to the aforementioned colloidal material. At a 10 kDa threshold for the ultrafiltration devices, it is likely that most of the RNA material, even if fragmented, is being captured. For example, the sequences for the primer and probes used in this study (Table 2) have a molecular range are 4.9-9.7 kDa (Stothard, 2000). It is improbable that the RNA being measured in the wastewater is of the exact length and therefore molecular weight of the primers and probes. Moreover, the RNA that is associated with solid and colloidal material would be larger and be adequately captured by the ultrafiltration devices used in this study. A greater concern is potential membrane adsorption (Ahmed et al., 2020) or clogging of the membrane.

2.4.2 Ultrafiltration Device Comparison

Direct comparison of the three ultrafiltration devices (Amicon Ultra-4, Amicon Ultra-15, and Centricon Plus-70) showed that they had different abilities to isolate SARS-CoV-2, PMMoV, and the seeded surrogates (229E, MHV) (Figure 7). Supply chain challenges experienced throughout this study limited the availability of different devices during the viral partitioning experiments (1-3) making it necessary to compare their performance directly. Although these devices have been used in other methods and compared indirectly as part of interlaboratory studies (Canadian Water Network, 2020; Chik et al., 2021; Pecson et al., 2021) a direct device comparison has not been reported in the literature to date (a far as we are aware).

While a direct comparison of the three ultrafiltration devices has not been reported in the literature, there have been some comparisons between the Amicon Ultra-15 and the Centricon Plus-70 devices. Ahmed et al. (2020) compared seeded MHV concentrations using opposing ultrafiltration brands with different membrane sizes: a 30 kDa Amicon Ultra-15 device and a 10 kDa Centricon Plus-70 device. Interestingly, the pre-filtration step (forms the pellet) using a centrifugal condition of 4,500 x *g* for 10 min (similar to Condition A) resulted in a 30% loss of MHV when comparing the ultrafiltration devices (Ahmed et al., 2020). Correspondingly, these data align with the data presented here as MHV (and SARS-CoV-2) were primarily in the supernatant fraction under Condition A (4,000 x *g*, 10 min, with brake). In contrast to this study, Ahmed et al. (2020) found the Amicon Ultra-15 device performed better than the Centricon Plus-70 device by 50%. The authors noted that inhibition was not present – eliminating the

inhibitor co-concentration concern – and that the loss could be due to adsorption to the membrane due to a greater surface area for the Centricon Plus-70 device. However, the design of the Centricon Plus-70 device (Figure A1) may have greater RNA yields for the studied gene targets over the Amicon devices as it enables the user to capture more of the particulate matter when the concentrate cup is inverted to collect the concentrate. Across the two experiments that compared the ultrafiltration devices (Figure 7), the surrogates (229E, MHV) detected that the Amicon Ultra-15 device underestimated viral RNA compared to the Amicon Ultra-4 and Centricon Plus-70 devices. Comparatively, this was in line with what was also observed with SARS-CoV-2 and PMMoV. With a method reliant on the Amicon Ultra-15 device, there is a risk that surveillance data for public health may be biased by the low performance of the device (at least under the conditions used in this study) as it can estimate lower than actual SARS-CoV-2 RNA concentrations in wastewater. Overall, there is evidence that ultrafiltration devices do not measure viral RNA equivalently (Figure 7) and great care should be taken to thoroughly test and optimize the methods used.

There are a few limitations to consider when comparing ultrafiltration devices. First, differences in membrane size should be tested as the 10 kDa can clog more readily. Depending on the matrix, this could be a factor to deal with when filtering with the devices. Testing different membrane sizes against each other would clarify if they can be used interchangeably (i.e., if 10 kDa garners comparable results as 30 kDa). There is some evidence that smaller membranes (down to 10 kDa) have performed marginally better than a larger membrane (up to 100 kDa) when measuring SARS-CoV-2 RNA (Boogaerts et al., 2021) but further testing should be done to verify these comparisons. Another aspect to consider is the ratio of surface area (cm^2) to process volume (mL). For the Amicon Ultra-4 device, the ratio between surface area and process volume is 0.75 (3 cm^2:4 mL) whereas the Amicon Ultra-15 device has a ratio of 0.51 (7.6 cm^2:15 mL) (Table A1). With a smaller surface area to process volume ratio, there may be an increased tendency to clog and trap RNA associated with particles that should otherwise remain in the concentrate.

2.4.3 Conclusion

In conclusion, the partitioning of SARS-CoV-2 RNA and related viruses is most appropriately described as apparent partitioning. With this in mind, SARS-CoV-2 RNA shows an even split between the supernatant (liquid) and pellet (solid) fractions under centrifugal conditions that are moderately hard and long (12,000 x *g*, 1.5 h, no brake). The implication of this is that a diverse suite of methods can quantify

SARS-CoV-2 since it is present in both fractions. Additionally, care must be taken when selecting ultrafiltration devices as they are not equivalent and may underestimate viral RNA in the supernatant (liquid) fraction under some conditions. Since PMMoV is morphologically different than SARS-CoV-2, and there is a difference in its apparent partitioning, it is recommended that care be taken with its use as a normalizer. Accordingly, further research is required to better characterize the partitioning kinetics of SARS-CoV-2 and related viruses in wastewater so methods can continue to be developed. Such research would address where these viruses are located in wastewater (adsorbed, embedded, or in solution) and if the viruses are intact, fragmented, or degraded before extracting them. The viruses 229E and MHV can be effective surrogates for SARS-CoV-2. With that said, care must be taken to consider the apparent partitioning of the surrogates to ensure it aligns more closely with SARS-CoV-2 in the selected analytical approach. Another key strength of using surrogates is benchmarking a method's performance and to flag potential inconsistencies. Finally, it is recommended that WBS programs reflect on the strengths and limitations of diverse methods to establish a foundation of best practices. Understanding the behaviour of viruses and surrogates is critical to the development of robust methods and interpretation of results and will help prepare for WBS applications to other emerging infectious diseases of concern.

Chapter 3
Conclusion and Recommendations

3.1 Conclusion

Wastewater-based surveillance (WBS) has become integral to supporting Public Health Units (PHUs) during the coronavirus disease (COVID-19) pandemic. The national collaboration between PHUs, government, academia, and private labs that have taken place in Canada has contributed to its success in the field (Hrudey et al., 2022). However, there continues to be a need to further develop and refine methods to measure SARS-CoV-2 RNA in wastewater. As there is no standardization of methods, challenges remain with the interpretation of wastewater surveillance data for COVID-19. Additionally, the virus SARS-CoV-2 has not remained static with the emergence of variants in late 2020. It is especially important to ensure that methods continue to measure SARS-CoV-2 RNA in wastewater in a consistent manner to ensure that robust data is supplied to PHUs and the public.

The data presented here indicate that SARS-CoV-2 RNA (as measured by N1 and N2 gene targets) in wastewater does not exclusively partition to the solid fraction in wastewater. Depending on the centrifugal conditions, the majority of the SARS-CoV-2 RNA may remain in the liquid fraction even when the centrifugation setting is harder (12,000 x *g*, 1.5 h, no brake). With that said, it is important to recognize that these partitioning patterns are considered apparent partitioning as it is largely dependent on the method's ability (centrifugation, ultrafiltration) to separate fractions and to measure the RNA within. This is further supported by the observation that ultrafiltration devices are not equivalent. Compared to the Amicon Ultra-4 and Centricon Plus-70 devices, there is evidence to suggest that the Amicon Ultra-15 device underestimates SARS-CoV-2 RNA in the liquid fraction of wastewater (under the conditions tested). Therefore, careful consideration should be applied for methods that rely on ultrafiltration devices as it may impact the underlying surveillance data for SARS-CoV-2 RNA.

3.2 Limitations

Across all experiments, sample sizes per treatment group were kept to four which can pose concerns if the few replicates are not precise. All experiments were designed to fit all of the samples onto a 96-well PCR plate to mitigate inter-plate variability while still maintaining qPCR controls on every plate (i.e., positive control, standard curve, NTC, NRT). Since the partitioning experiments (1-3) were replicated four times (Figure 4-6) and the ultrafiltration device comparisons twice (Experiment 4A/B; Figure 7), confidence

across them was established. Moreover, these data were consistent at different periods in the year when different SARS-CoV-2 variants were circulating. It was also important to capture the shift in apparent partitioning in the same experiment to avoid confounding factors such as matrix effects, potential handling differences, or aging of the wastewater sample. In doing so, partitioning experiments were challenged by sample independence since the supernatant (liquid) and pellet (solid) fractions originate from the same conical tube. However, this is seen as a strength since the apparent partitioning can be captured per sample instead of an estimate from unlinked fractions which would confound how apparent partitioning is reflected. Statistically, the methods to measure the supernatant (liquid) and pellet (solid) fractions were considered different. Moreover, the wastewater sample itself is considered random with 40 mL aliquots randomly assigned following a thorough mixing. Overall, the replication of experiments is a key strength of this study and increases confidence in the results and conclusions.

Limitations of Experiment 4A/B include testing the devices under Condition B (12,000 x *g*, 1.5 h, no brake) and with a 10 kDa membrane size as the only experimental treatment. It has been reported that a decrease in membrane size (down to 10 kDa) had only a minor improvement over larger membranes (up to 100 kDa) for measuring SARS-CoV-2 RNA and that the higher membrane size may mitigate co-concentration of PCR inhibitors (Boogaerts et al., 2021). Therefore, it is unlikely that the membrane size had a major effect on the RNA concentrations for the ultrafiltration comparison, especially since there was no indication of qPCR inhibition as previously mentioned. Additionally, it is hypothesized that these results (Experiment 4A/B; Figure 7) would hold under other conditions (e.g., Condition A; 4,000 x *g*, 10 min, with brake) since the apparent partitioning (Experiments 1-3) trends aligned with what was observed by the head-to-head comparison of the ultrafiltration devices. For example, the Amicon Ultra-4 and Centricon Plus-70 devices showed an even split of RNA copies for SARS-CoV-2 and the surrogates under Condition B (12,000 x *g*, 1.5 h, no brake) suggesting that they should be comparable devices. Conversely, the Amicon Ultra-15 device indicated a pellet (solids) dominance for the surrogates, a lower-than-expected PMMoV signal with SARS-CoV-2 being non-quantifiable due in part to the low total signal in the wastewater at that time. Therefore, the data from the partitioning experiments (1-3; Figure 4-6) align with the direct head-to-head ultrafiltration device comparison (Experiment 4A/B; Figure 7). Finally, the sub-sampling from the same tube for both the Amicon Ultra-4 and Ultra-15 devices introduces an independence concern for the liquid-based concentration method. However, given the observations of lower-than-expected RNA copies in the supernatant (liquid) with the Amicon Ultra-15 device (Experiment 2), it is unlikely that sampling from the same tube is the source of the difference

between the two ultrafiltration devices. Moreover, using the same sample offers a direct comparison from within that sample. For future iterations of this experiment, all three ultrafiltration devices should be used to measure the RNA from one wastewater sample and separate individual wastewater samples. Overall, this study demonstrates that ultrafiltration devices are not equivalent and that Amicon Ultra-15 devices, under the conditions tested, significantly underestimated viral RNA from wastewater samples.

3.3 Recommendations

There are several key recommendations based on the data presented:

1. *Further study of the fate of SARS-CoV-2 in wastewater*. While this study demonstrated the importance of the apparent partitioning of SARS-CoV-2 RNA in wastewater, there remains a need to elucidate the partitioning of SARS-CoV-2 in wastewater. A confounding factor that challenges the study of SARS-CoV-2 RNA partitioning is the state at which SARS-CoV-2 exists in wastewater. Whether it is intact, fragmented, or degraded and to what extent it is adsorbed or encapsulated by organic matter is still largely unknown. Moreover, different matrices may also affect the partitioning behaviour of SARS-CoV-2 and understanding this process is important for understanding its fate in wastewater. New data into the partitioning of SARS-CoV-2 and other viruses that are important for human health will contribute to the improvement of methods for WBS.
2. *Continue to refine and develop methods that are tailored to viruses that can be measured in wastewater*. Since the apparent partitioning of SARS-CoV-2 RNA in wastewater splits between the solid and liquid fractions, a method that can capture RNA from both fractions is ideal. The use of PEG precipitation followed by high-speed centrifugation for wastewater samples used in this study improved recovery over the solids-only-based approach. However, based on the total amount of RNA for the tested gene targets (N1, N2, PMMoV, 229E, MHV) in the wastewater sample, there is still room to improve the recovery from both fractions at once. New innovative methods that are better suited to measure RNA from a whole wastewater sample should be further studied and validated to ensure its place among acceptable methods. Moreover, this may address some of the concerns that arise from using an endogenous reference such as PMMoV that exhibits different apparent partitioning behaviour than SARS-CoV-2. With this in mind, all assumptions need to be carefully validated. Many of the methods deployed during the pandemic were adopted rapidly and there was a reluctance to change once

trends had been established. New methods with improved accuracy and precision will make WBS an even more powerful tool in the future.

3. *Implementation of surrogates in WBS programs*. While it may be impossible to find an exogenous surrogate that perfectly reflects SARS-CoV-2 behaviour in wastewater, this study has demonstrated that it is possible to have a surrogate that aligns closely with SARS-CoV-2. For a surrogate to best be utilized, it is important that the apparent partitioning behaviour is considered, and the surrogates are used with care and caution under strict protocols. Furthermore, surrogates can act as an important QA/QC measure for the overall method by flagging samples that may not have been concentrated, extracted, or quantified properly.
4. *Develop a foundation of methodological best practices*. Each of the above recommendations supports the notion of refining and developing methods to better serve WBS therein turn supporting PHUs to better monitor pathogens in a community. For the field to continue to be successful, the benefits and drawbacks of each method need to be explicitly outlined for public health officials to consider in their interpretation. For surveillance, there must be consistency in the methods to extract the virus to ensure the reliability of the data.

References

Aguado, D., Fores, E., Guerrero-Latorre, L., Rusiñol, M., Martínez-Puchol, S., Codony, F., Girones, R., & Bofill-Mas, S. (2019). VirWaTest, a point-of-use method for the detection of viruses in water samples. *Journal of Visualized Experiments*, *2019*(147), 1–9. https://doi.org/10.3791/59463

Aguiar-Oliveira, M. de L., Campos, A., R. Matos, A., Rigotto, C., Sotero-Martins, A., Teixeira, P. F. P., & Siqueira, M. M. (2020). Wastewater-based epidemiology (WBE) and viral detection in polluted surface water: A valuable tool for COVID-19 surveillance—A brief review. *International Journal of Environmental Research and Public Health*, *17*(24), 9251. https://doi.org/10.3390/ijerph17249251

Ahmed, W., Bertsch, P. M., Bivins, A., Bibby, K., Farkas, K., Gathercole, A., Haramoto, E., Gyawali, P., Korajkic, A., McMinn, B. R., Mueller, J. F., Simpson, S. L., Smith, W. J. M., Symonds, E. M., Thomas, K. V, Verhagen, R., & Kitajima, M. (2020). Comparison of virus concentration methods for the RT-qPCR-based recovery of murine hepatitis virus, a surrogate for SARS-CoV-2 from untreated wastewater. *Science of The Total Environment*, *739*, 139960. https://doi.org/10.1016/j.scitotenv.2020.139960

Ai, Y., Davis, A., Jones, D., Lemeshow, S., Tu, H., He, F., Ru, P., Pan, X., Bohrerova, Z., & Lee, J. (2021). Wastewater SARS-CoV-2 monitoring as a community-level COVID-19 trend tracker and variants in Ohio, United States. *Science of the Total Environment*, *801*, 149757. https://doi.org/10.1016/j.scitotenv.2021.149757

Aptel, P., & Clifton, M. (1986). Ultrafiltration. In *Synthetic Membranes: Science, Engineering and Applications* (pp. 249–305). Springer Netherlands. https://doi.org/10.1007/978-94-009-4712-2_10

Aquino De Carvalho, N., Stachler, E. N., Cimabue, N., & Bibby, K. (2017). Evaluation of Phi6 persistence and suitability as an enveloped virus surrogate. *Environmental Science and Technology*, *51*(15), 8692–8700. https://doi.org/10.1021/acs.est.7b01296

Artika, I. M., Dewantari, A. K., & Wiyatno, A. (2020). Molecular biology of coronaviruses: Current knowledge. *Heliyon*, *6*(8), e04743. https://doi.org/10.1016/j.heliyon.2020.e04743

Atha, D. H., & Ingham, K. C. (1981). Mechanism of precipitation of proteins by polyethylene glycols: Analysis in terms of excluded volume. *Journal of Biological Chemistry*, *256*(23), 12108–12117. https://doi.org/10.1016/S0021-9258(18)43240-1

Barril, P. A., Pianciola, L. A., Mazzeo, M., Ousset, M. J., Jaureguiberry, M. V., Alessandrello, M., Sánchez, G., & Oteiza, J. M. (2021). Evaluation of viral concentration methods for SARS-CoV-2 recovery from wastewaters. *Science of the Total Environment*, *756*, 144105. https://doi.org/10.1016/j.scitotenv.2020.144105

Basha, M. (2020). Centrifugation. In *Analytical Techniques in Biochemistry* (pp. 13–21). Springer US. https://doi.org/10.1007/978-1-0716-0134-1_3

Belhaouari, D. B., Wurtz, N., Grimaldier, C., Lacoste, A., Pires de Souza, G. A., Penant, G., Hannat, S., Baudoin, J.-P., & La Scola, B. (2021). Microscopic observation of SARS-like particles in RT-qPCR SARS-CoV-2 positive sewage samples. *Pathogens*, *10*(5), 516. https://doi.org/10.3390/pathogens10050516

Boehm, A. B., Hughes, B., Doung, D., Chan-Herur, V., Buchman, A., Wolfe, M. K., & White, B. J. (2022). Wastewater surveillance of human influenza, metapneumovirus, parainfluenza, respiratory syncytial virus (RSV), rhinovirus, and seasonal coronaviruses during the COVID-19 pandemic. *medRxiv*, 2022.09.22.22280218. https://doi.org/10.1101/2022.09.22.22280218

Boni, L. T., Stewart, T. P., Alderfer, J. L., & Hui, S. W. (1981). Lipid-polyethylene glycol interactions: II. Formation of defects in bilayers. *The Journal of Membrane Biology*, *62*(1–2), 71–77. https://doi.org/10.1007/BF01870201

Boogaerts, T., Jacobs, L., De Roeck, N., Van den Bogaert, S., Aertgeerts, B., Lahousse, L., van Nuijs, A. L. N., & Delputte, P. (2021). An alternative approach for bioanalytical assay optimization for wastewater-based epidemiology of SARS-CoV-2. *Science of the Total Environment*, *789*, 148043. https://doi.org/10.1016/j.scitotenv.2021.148043

Burnet, J.-B., Cauchie, H.-M., Walczak, C., Goeders, N., & Ogorzaly, L. (2023). Persistence of endogenous RNA biomarkers of SARS-CoV-2 and PMMoV in raw wastewater: Impact of temperature and implications for wastewater-based epidemiology. *Science of The Total Environment, 857,* 159401. https://doi.org/10.1016/j.scitotenv.2022.159401

Cai, P., Huang, Q. Y., & Zhang, X. W. (2006). Interactions of DNA with clay minerals and soil colloidal particles and protection against degradation by DNase. *Environmental Science and Technology*, *40*(9), 2971–2976. https://doi.org/10.1021/es0522985

Canadian Water Network. (2020). *Phase I Inter-Laboratory Study: Comparison of approaches to quantify*

SARS-CoV-2 RNA in wastewater. https://cwn-rce.ca/covid-19-wastewater-coalition/ phase-1-inter-laboratory-study

Cao, Y., Griffith, J. F., Dorevitch, S., & Weisberg, S. B. (2012). Effectiveness of qPCR permutations, internal controls and dilution as means for minimizing the impact of inhibition while measuring *Enterococcus* in environmental waters. *Journal of Applied Microbiology*, *113*(1), 66–75. https://doi.org/10.1111/j.1365-2672.2012.05305.x

Casanova, L., Rutala, W. A., Weber, D. J., & Sobsey, M. D. (2009). Survival of surrogate coronaviruses in water. *Water Research*, *43*(7), 1893–1898. https://doi.org/10.1016/j.watres.2009.02.002

Castiglioni, S., Bijlsma, L., Covaci, A., Emke, E., Hernandez, F., Reid, M., Ort, C., Thomas, K. V, van Nuijs, A. L. N., de Voogt, P., & Zuccato, E. (2013). Evaluation of uncertainties associated with the determination of community drug use through the measurement of sewage drug biomarkers. *Environmental Science & Technology*, *47*(3), 1452–1460. https://doi.org/10.1021/es302722f

Ceban, F., Ling, S., Lui, L. M. W., Lee, Y., Gill, H., Teopiz, K. M., Rodrigues, N. B., Subramaniapillai, M., Di Vincenzo, J. D., Cao, B., Lin, K., Mansur, R. B., Ho, R. C., Rosenblat, J. D., Miskowiak, K. W., Vinberg, M., Maletic, V., & McIntyre, R. S. (2022). Fatigue and cognitive impairment in Post-COVID-19 Syndrome: A systematic review and meta-analysis. *Brain, Behavior, and Immunity*, *101*, 93–135. https://doi.org/10.1016/j.bbi.2021.12.020

Centers for Disease Control and Prevention. (2020, April 10). *Research use only 2019-novel coronavirus (2019-nCoV) real-time RT-PCR primer and probe information*. Retrieved December 13, 2022, from https://web.archive.org/web/20200506150010/https://www.cdc.gov/coronavirus/2019-ncov/lab/rt-pcr-panel-primer-probes.html

Centers for Disease Control and Prevention. (2022a, April 26). *SARS-CoV-2 variant classifications and definitions*. Retrieved December 13, 2022, from https://www.cdc.gov/coronavirus/2019-ncov/variants/variant-classifications.html

Centers for Disease Control and Prevention. (2022b, October 26). *Symptoms of COVID-19*. Retrieved December 13, 2022, from https://www.cdc.gov/coronavirus/2019-ncov/symptoms-testing/symptoms.html

Centers for Disease Control and Prevention. (2022c, December 16). *Long COVID or post-COVID conditions*. Retrieved December 21, 2022, from https://www.cdc.gov/coronavirus/2019-ncov/long-

term-effects/index.html

Chik, A. H. S., Glier, M. B., Servos, M., Mangat, C. S., Pang, X.-L., Qiu, Y., D'Aoust, P. M., Burnet, J.-B., Delatolla, R., Dorner, S., Geng, Q., Giesy, J. P., McKay, R. M., Mulvey, M. R., Prystajecky, N., Srikanthan, N., Xie, Y., Conant, B., & Hrudey, S. E. (2021). Comparison of approaches to quantify SARS-CoV-2 in wastewater using RT-qPCR: Results and implications from a collaborative inter-laboratory study in Canada. *Journal of Environmental Sciences*, *107*, 218–229. https://doi.org/10.1016/j.jes.2021.01.029

Cordova, A., Deserno, M., Gelbart, W. M., & Ben-Shaul, A. (2003). Osmotic shock and the strength of viral capsids. *Biophysical Journal*, *85*(1), 70–74. https://doi.org/10.1016/S0006-3495(03)74455-5

D'Aoust, P. M., Mercier, E., Montpetit, D., Jia, J. J., Alexandrov, I., Neault, N., Baig, A. T., Mayne, J., Zhang, X., Alain, T., Langlois, M. A., Servos, M. R., MacKenzie, M., Figeys, D., MacKenzie, A. E., Graber, T. E., & Delatolla, R. (2021). Quantitative analysis of SARS-CoV-2 RNA from wastewater solids in communities with low COVID-19 incidence and prevalence. *Water Research*, *188*, 116560. https://doi.org/10.1016/j.watres.2020.116560

Dhiyebi, H., Cheng, L., Varia, M., Atanas, K., Srikanthan, N., Hayat, S., Ikert, H., Fuzzen, M., Sing-Judge, C., Badlani, Y., Zeeb, E., Bragg, L., Delatolla, R., Giesy, J., Gilliland, E., & Servos, M. (2023a). Estimation of COVID-19 case incidence during the Omicron outbreaks based on SARS-CoV-2 wastewater load in previous waves, Peel Region, Canada. *Emerging Infectious Diseases [in review]*.

Dhiyebi, H., Farah, J. A., Ikert, H., Srikanthan, N., Hayat, S., Bragg, L., Qasim, A., Payne, M., Kaleis, L., Paget, C., Celmer-Repin, D., Folkema, A., Drew, S., Delatolla, R., Giesy, J. P., & Servos, M. R. (2023b). Assessment of seasonality and normalization techniques for wastewater-based surveillancein Ontario, Canada. *Frontiers in Public Health [in review]*.

Dreier, J., Störmer, M., & Kleesiek, K. (2005). Use of bacteriophage MS2 as an internal control in viral reverse transcription-PCR assays. *Journal of Clinical Microbiology*, *43*(9), 4551–4557. https://doi.org/10.1128/JCM.43.9.4551-4557.2005

Feng, S., Roguet, A., McClary-Gutierrez, J. S., Newton, R. J., Kloczko, N., Meiman, J. G., & McLellan, S. L. (2021). Evaluation of sampling, analysis, and normalization methods for SARS-CoV-2 concentrations in wastewater to assess COVID-19 burdens in Wisconsin communities. *ACS ES&T*

Water, *1*(8), 1955–1965. https://doi.org/10.1021/acsestwater.1c00160

Government of Canada. (2022, December 12). *COVID-19: Outbreak update*. Retrieved December 13, 2022, from https://www.canada.ca/en/public-health/services/diseases/2019-novel-coronavirus-infection.html

Graham, K. E., Loeb, S. K., Wolfe, M. K., Catoe, D., Sinnott-Armstrong, N., Kim, S., Yamahara, K. M., Sassoubre, L. M., Mendoza Grijalva, L. M., Roldan-Hernandez, L., Langenfeld, K., Wigginton, K. R., & Boehm, A. B. (2021). SARS-CoV-2 RNA in wastewater settled solids is associated with COVID-19 cases in a large urban sewershed. *Environmental Science and Technology*, *55*(1), 488–498. https://doi.org/10.1021/acs.est.0c06191

Heijnen, L., & Medema, G. (2011). Surveillance of influenza A and the pandemic influenza A (H1N1) 2009 in sewage and surface water in the Netherlands. *Journal of Water and Health*, *9*(3), 434–442. https://doi.org/10.2166/wh.2011.019

Hellmer, M., Paxeus, N., & Norder, H. (2014). Detection of pathogenic viruses in sewage provided early warnings of hepatitis A virus and norovirus outbreaks. *Applied and Environmental Microbiology*, *80*(21), 6771–6781. https://doi.org/10.1128/AEM.01981-14

Hendriksen, R. S., Munk, P., Njage, P., van Bunnik, B., McNally, L., Lukjancenko, O., Roder, T., Nieuwenhuijse, D., Pedersen, S. K., Kjeldgaard, J., Kaas, R. S., Clausen, P., Vogt, J. K., Leekitcharoenphon, P., van de Schans, M. G. M., Zuidema, T., Husman, A. M. D., Rasmussen, S., Petersen, B., … Surveillance, G. S. (2019). Global monitoring of antimicrobial resistance based on metagenomics analyses of urban sewage. *Nature Communications*, *10*. https://doi.org/10.1038/s41467-019-08853-3

Hill, K., Zamyadi, A., Deere, D., Vanrolleghem, P. A., & Crosbie, N. D. (2021). SARS-CoV-2 known and unknowns, implications for the water sector and wastewater-based epidemiology to support national responses worldwide: Early review of global experiences with the COVID-19 pandemic. *Water Quality Research Journal*, *56*(2), 57–67. https://doi.org/10.2166/wqrj.2020.100

Hokajärvi, A. M., Rytkönen, A., Tiwari, A., Kauppinen, A., Oikarinen, S., Lehto, K. M., Kankaanpää, A., Gunnar, T., Al-Hello, H., Blomqvist, S., Miettinen, I. T., Savolainen-Kopra, C., & Pitkänen, T. (2021). The detection and stability of the SARS-CoV-2 RNA biomarkers in wastewater influent in Helsinki, Finland. *Science of the Total Environment*, *770*, 145274.

https://doi.org/10.1016/j.scitotenv.2021.145274

Hrudey, S. E., Ashbolt, N. J., Isaac-Renton, J. L., McKay, R. M., & Servos, M. R. (2020). Wastewater-based epidemiology for SARS-CoV-2. *Royal Society of Canada*, *23*, 1–6. https://rsc-src.ca/en/voices/epidemiology-for-sars-cov-2

Hrudey, S. E., Bischel, H. N., Charrois, J., Chik, A. H. S., Conant, B., Delatolla, R., Dorner, S., Graber, T., Hubert, C., Isaac-Renton, J., Pons, W., Safford, H., Servos, M., & Sikora, C. (2022). *Wastewater Surveillance for SARS-CoV-2 RNA in Canada (August 2022)*. Royal Society of Canada. https://rsc-src.ca/en/covid-19-policy-briefing/wastewater-surveillance-for-sars-cov-2-rna-in-canada

Hsu, S.-Y., Bayati, M., Li, C., Hsieh, H.-Y., Belenchia, A., Klutts, J., Zemmer, S. A., Reynolds, M., Semkiw, E., Johnson, H.-Y., Foley, T., Wieberg, C. G., Wenzel, J., Johnson, M. C., & Lin, C.-H. (2022). Biomarkers selection for population normalization in SARS-CoV-2 wastewater-based epidemiology. *Water Research*, *223*, 118985. https://doi.org/10.1016/j.watres.2022.118985

Hughes, B., Duong, D., White, B. J., Wigginton, K. R., Chan, E. M. G., Wolfe, M. K., & Boehm, A. B. (2022). Respiratory syncytial virus (RSV) RNA in wastewater settled solids reflects RSV clinical positivity rates. *Environmental Science and Technology Letters*, *9*(2), 173–178. https://doi.org/10.1021/acs.estlett.1c00963

International Committee on Taxonomy of Viruses. (2021, July). *Virus Taxonomy: 2021 release, EC 53*. Retrieved January 27, 2023, from https://ictv.global/taxonomy

Islam, G., Gedge, A., Lara-Jacobo, L., Kirkwood, A., Simmons, D., & Desaulniers, J. P. (2022). Pasteurization, storage conditions and viral concentration methods influence RT-qPCR detection of SARS-CoV-2 RNA in wastewater. *Science of the Total Environment*, *821*, 153228. https://doi.org/10.1016/j.scitotenv.2022.153228

Jeong, H. W., Kim, S. M., Kim, H. S., Kim, Y. Il, Kim, J. H., Cho, J. Y., Kim, S. hyung, Kang, H., Kim, S. G., Park, S. J., Kim, E. H., & Choi, Y. K. (2020). Viable SARS-CoV-2 in various specimens from COVID-19 patients. *Clinical Microbiology and Infection*, *26*(11), 1520–1524. https://doi.org/10.1016/j.cmi.2020.07.020

Kim, S., Kennedy, L. C., Wolfe, M. K., Criddle, C. S., Duong, D. H., Topol, A., White, B. J., Kantor, R. S., Nelson, K. L., Steele, J. A., Langlois, K., Griffith, J. F., Zimmer-Faust, A. G., McLellan, S. L., Schussman, M. K., Ammerman, M., Wigginton, K. R., Bakker, K. M., & Boehm, A. B. (2022).

SARS-CoV-2 RNA is enriched by orders of magnitude in primary settled solids relative to liquid wastewater at publicly owned treatment works. *Environmental Science: Water Research and Technology*, *8*(4), 757–770. https://doi.org/10.1039/d1ew00826a

Kitajima, M., Sassi, H. P., & Torrey, J. R. (2018). Pepper mild mottle virus as a water quality indicator. *npj Clean Water*, *1*(1). https://doi.org/10.1038/s41545-018-0019-5

Kitamura, K., Sadamasu, K., Muramatsu, M., & Yoshida, H. (2021). Efficient detection of SARS-CoV-2 RNA in the solid fraction of wastewater. *Science of the Total Environment*, *763*, 144587. https://doi.org/10.1016/j.scitotenv.2020.144587

La Rosa, G., Bonadonna, L., Lucentini, L., Kenmoe, S., & Suffredini, E. (2020). Coronavirus in water environments: Occurrence, persistence and concentration methods - A scoping review. *Water Research*, *179*, 115899. https://doi.org/10.1016/j.watres.2020.115899

Lago, P. M., Gary, H. E., Perez, L. S., Caceres, V., Olivera, J. B., Puentes, R. P., Corredor, M. B., Jimenez, P., Pallansch, M. A., & Cruz, R. G. (2003). Poliovirus detection in wastewater and stools following an immunization campaign in Havana, Cuba. *International Journal of Epidemiology*, *32*(5), 772–777. https://doi.org/10.1093/ije/dyg185

LaTurner, Z. W., Zong, D. M., Kalvapalle, P., Gamas, K. R., Terwilliger, A., Crosby, T., Ali, P., Avadhanula, V., Santos, H. H., Weesner, K., Hopkins, L., Piedra, P. A., Maresso, A. W., & Stadler, L. B. (2021). Evaluating recovery, cost, and throughput of different concentration methods for SARS-CoV-2 wastewater-based epidemiology. *Water Research*, *197*, 117043. https://doi.org/10.1016/j.watres.2021.117043

Leung, W. W.-F. (2020). Principles of centrifugal sedimentation. In *Centrifugal Separations in Biotechnology* (pp. 27–48). Elsevier. https://doi.org/10.1016/B978-0-08-102634-2.00002-7

Manuel, D. G., Amadei, C. A., Campbell, J. R., Brault, J.-M., Zierler, A., & Veillard, J. (2022). *Strengthening public health surveillance through wastewater testing: An essential investment for the COVID-19 pandemic*. World Bank. https://openknowledge.worldbank.org/handle/10986/36852

Markt, R., Mayr, M., Peer, E., Wagner, A. O., Lackner, N., & Insam, H. (2021). Detection and stability of SARS-CoV-2 fragments in wastewater: Impact of storage temperature. *Pathogens*, *10*(9), 4–7. https://doi.org/10.3390/pathogens10091215

Mathieu, E., Ritchie, H., Ortiz-Ospina, E., Roser, M., Hasell, J., Appel, C., Giattino, C., & Rodés-Guirao,

L. (2021). A global database of COVID-19 vaccinations. *Nature Human Behaviour*, *5*(7), 947–953. https://doi.org/10.1038/s41562-021-01122-8

Mathieu, E., Ritchie, H., Rodés-Guirao, L., Appel, C., Giattino, C., Hasell, J., Macdonald, B., Dattani, S., Beltekian, D., Ortiz-Ospina, E., & Roser, M. (2020). *Coronavirus Pandemic (COVID-19)*. Our World in Data. Retrieved December 13, 2022, from https://ourworldindata.org/coronavirus

McCarty, P. L., & Aieta, E. M. (1984). Chemical indicators and surrogate parameters in water treatment. *Journal American Water Works Association*, *76*(10), 98–106. https://www.jstor.org/stable/41273063

Medema, G., Heijnen, L., Elsinga, G., Italiaander, R., & Brouwer, A. (2020). Presence of SARS-CoV-2 RNA in sewage and correlation with reported COVID-19 prevalence in the early stage of the epidemic in the Netherlands. *Environmental Science & Technology Letters*, *7*(7), 511–516. https://doi.org/10.1021/acs.estlett.0c00357

Mercier, E., D'Aoust, P. M., Thakali, O., Hegazy, N., Jia, J. J., Zhang, Z., Eid, W., Plaza-Diaz, J., Kabir, M. P., Fang, W., Cowan, A., Stephenson, S. E., Pisharody, L., MacKenzie, A. E., Graber, T. E., Wan, S., & Delatolla, R. (2022). Municipal and neighbourhood level wastewater surveillance and subtyping of an influenza virus outbreak. *Scientific Reports*, *12*(1), 1–11. https://doi.org/10.1038/s41598-022-20076-z

Michael-Kordatou, I., Karaolia, P., & Fatta-Kassinos, D. (2020). Sewage analysis as a tool for the COVID-19 pandemic response and management: the urgent need for optimised protocols for SARS-CoV-2 detection and quantification. *Journal of Environmental Chemical Engineering*, *8*(5), 104306. https://doi.org/10.1016/j.jece.2020.104306

Ministry of the Environment, Conservation and Parks. (2022, September 16). *COVID-19 wastewater monitoring*. Retrieved February 12, 2023, from https://www.ontario.ca/page/covid-19-wastewater-monitoring

Mondal, S., Feirer, N., Brockman, M., Preston, M. A., Teter, S. J., Ma, D., Goueli, S. A., Moorji, S., Saul, B., & Cali, J. J. (2021). A direct capture method for purification and detection of viral nucleic acid enables epidemiological surveillance of SARS-CoV-2. *Science of the Total Environment*, *795*, 148834. https://doi.org/10.1016/j.scitotenv.2021.148834

Pecson, B. M., Darby, E., Haas, C. N., Amha, Y. M., Bartolo, M., Danielson, R., Dearborn, Y., Di Giovanni, G., Ferguson, C., Fevig, S., Gaddis, E., Gray, D., Lukasik, G., Mull, B., Olivas, L.,

Olivieri, A., Qu, Y., & SARS-CoV-2 Interlaboratory Consortium. (2021). Reproducibility and sensitivity of 36 methods to quantify the SARS-CoV-2 genetic signal in raw wastewater: Findings from an interlaboratory methods evaluation in the U.S. *Environmental Science: Water Research & Technology*, *7*(3), 504–520. https://doi.org/10.1039/D0EW00946F

Philo, S. E., Keim, E. K., Swanstrom, R., Ong, A. Q. W., Burnor, E. A., Kossik, A. L., Harrison, J. C., Demeke, B. A., Zhou, N. A., Beck, N. K., Shirai, J. H., & Meschke, J. S. (2021). A comparison of SARS-CoV-2 wastewater concentration methods for environmental surveillance. *Science of the Total Environment*, *760*, 144215. https://doi.org/10.1016/j.scitotenv.2020.144215

Poison, A. (1977). A theory for the displacement of proteins and viruses with polyethylene glycol. *Preparative Biochemistry*, *7*(2), 129–154. https://doi.org/10.1080/00327487708061631

Public Health Ontario. (2022). *Epidemiologic summary: SARS-CoV-2 whole genome sequencing in Ontario, March 1, 2022* (p. 4). Queen's Printer for Ontario. https://www.publichealthontario.ca/-/media/documents/ncov/epi/covid-19-sars-cov2-whole-genome-sequencing-epi-summary.pdf

Public Health Ontario. (2023). *Weekly epidemiologic summary: COVID-19 in Ontario – January 15 to January 21, 2023* (p. 23). King's Printer for Ontario. https://www.publichealthontario.ca/-/media/Documents/nCoV/epi/covid-19-weekly-epi-summary-report.pdf?rev=6c23fc74f3d14048ae40441966d1505e&sc_lang=en

R Core Team. (2021). *R: A Language and Environment for Statistical Computing*. https://www.r-project.org/

Raaben, M., Einerhand, A. W. C., Taminiau, L. J. A., Van Houdt, M., Bouma, J., Raatgeep, R. H., Büller, H. A., De Haan, C. A. M., & Rossen, J. W. A. (2007). Cyclooxygenase activity is important for efficient replication of mouse hepatitis virus at an early stage of infection. *Virology Journal*, *4*, 1–5. https://doi.org/10.1186/1743-422X-4-55

Rahimi, N. R., Fouladi-Fard, R., Aali, R., Shahryari, A., Rezaali, M., Ghafouri, Y., Ghalhari, M. R., Asadi-Ghalhari, M., Farzinnia, B., Conti Gea, O., & Fiore, M. (2021). Bidirectional association between COVID-19 and the environment: A systematic review. *Environmental Research*, *194*, 110692. https://doi.org/10.1016/j.envres.2020.110692

Respiratory Virus Infections Working Group. (2020). Canadian Public Health Laboratory Network: Prioritized support for northern, remote and isolated communities in Canada. *Canada*

Communicable Disease Report, *46*(10), 322–323. https://doi.org/10.14745/ccdr.v46i10a02

Robinson, C. A., Hsieh, H. Y., Hsu, S. Y., Wang, Y., Salcedo, B. T., Belenchia, A., Klutts, J., Zemmer, S., Reynolds, M., Semkiw, E., Foley, T., Wan, X. F., Wieberg, C. G., Wenzel, J., Lin, C. H., & Johnson, M. C. (2022). Defining biological and biophysical properties of SARS-CoV-2 genetic material in wastewater. *Science of the Total Environment*, *807*, 150786. https://doi.org/10.1016/j.scitotenv.2021.150786

Röder, B., Frühwirth, K., Vogl, C., Wagner, M., & Rossmanith, P. (2010). Impact of long-term storage on stability of standard DNA for nucleic acid-based methods. *Journal of Clinical Microbiology*, *48*(11), 4260–4262. https://doi.org/10.1128/JCM.01230-10

Roy, D. N., Biswas, M., Islam, E., & Azam, M. S. (2022). Potential factors influencing COVID-19 vaccine acceptance and hesitancy: A systematic review. *PLOS ONE*, *17*(3), e0265496. https://doi.org/10.1371/journal.pone.0265496

Safford, H. R., Shapiro, K., & Bischel, H. N. (2022). Opinion: Wastewater analysis can be a powerful public health tool—If it's done sensibly. *Proceedings of the National Academy of Sciences*, *119*(6), e2119600119. https://doi.org/10.1073/pnas.2119600119

Schoeman, D., & Fielding, B. C. (2019). Coronavirus envelope protein: Current knowledge. *Virology Journal*, *16*(1), 69. https://doi.org/10.1186/s12985-019-1182-0

Shieh, Y.-S. C., Wait, D., Tai, L., & Sobsey, M. D. (1995). Methods to remove inhibitors in sewage and other fecal wastes for enterovirus detection by the polymerase chain reaction. *Journal of Virological Methods*, *54*(1), 51–66. https://doi.org/10.1016/0166-0934(95)00025-P

Simpson, A., Topol, A., White, B. J., Wolfe, M. K., Wigginton, K. R., & Boehm, A. B. (2021). Effect of storage conditions on SARS- CoV-2 RNA quantification in wastewater solids. *PeerJ*, *9*, e11933. https://doi.org/10.7717/peerj.11933

Sinclair, R. G., Rose, J. B., Hashsham, S. A., Gerba, C. P., & Haase, C. N. (2012). Criteria for selection of surrogates used to study the fate and control of pathogens in the environment. *Applied and Environmental Microbiology*, *78*(6), 1969–1977. https://doi.org/10.1128/AEM.06582-11

Stothard, P. (2000). The sequence manipulation suite: JavaScript programs for analyzing and formatting protein and DNA sequences. *BioTechniques*, *28*(6), 1102–1104. https://doi.org/10.2144/00286ir01

Swango, K. L., Timken, M. D., Chong, M. D., & Buoncristiani, M. R. (2006). A quantitative PCR assay for the assessment of DNA degradation in forensic samples. *Forensic Science International*, *158*(1), 14–26. https://doi.org/10.1016/j.forsciint.2005.04.034

Torii, S., Furumai, H., & Katayama, H. (2021). Applicability of polyethylene glycol precipitation followed by acid guanidinium thiocyanate-phenol-chloroform extraction for the detection of SARS-CoV-2 RNA from municipal wastewater. *Science of The Total Environment*, *756*, 143067. https://doi.org/10.1016/j.scitotenv.2020.143067

United Nations. (2021, April 16). *Vaccine equity the 'challenge of our time', WHO chief declares, as governments call for solidarity, sharing*. Retrieved July 29, 2021, from https://news.un.org/en/story/2021/04/1089972

van Mulukom, V., Pummerer, L. J., Alper, S., Bai, H., Čavojová, V., Farias, J., Kay, C. S., Lazarevic, L. B., Lobato, E. J. C., Marinthe, G., Pavela Banai, I., Šrol, J., & Žeželj, I. (2022). Antecedents and consequences of COVID-19 conspiracy beliefs: A systematic review. *Social Science & Medicine*, *301*, 114912. https://doi.org/10.1016/j.socscimed.2022.114912

Vijgen, L., Keyaerts, E., Moës, E., Maes, P., Duson, G., & Van Ranst, M. (2005). Development of one-step, real-time, quantitative reverse transcriptase PCR assays for absolute quantitation of human coronaviruses OC43 and 229E. *Journal of Clinical Microbiology*, *43*(11), 5452–5456. https://doi.org/10.1128/JCM.43.11.5452-5456.2005

Wellings, F. M., Lewis, A. L., & Mountain, C. W. (1976). Demonstration of solids associated virus in wastewater and sludge. *Applied and Environmental Microbiology*, *31*(3), 354–358. https://doi.org/10.1128/aem.31.3.354-358.1976

Wilson, I. G. (1997). Inhibition and facilitation of nucleic acid amplification. *Applied and Environmental Microbiology*, *63*(10), 3741–3751. https://doi.org/10.1128/aem.63.10.3741-3751.1997

World Health Organization. (2020a, January 5). *Pneumonia of unknown cause – China*. Retrieved July 11, 2021, from https://web.archive.org/web/20200107032945/http:/www.who.int/csr/don/05-january-2020-pneumonia-of-unkown-cause-china/en/

World Health Organization. (2020b, January 9). *WHO Statement regarding cluster of pneumonia cases in Wuhan, China*. Retrieved July 11, 2021, from https://www.who.int/china/news/detail/09-01-2020-who-statement-regarding-cluster-of-pneumonia-cases-in-wuhan-china

World Health Organization. (2020c, March 11). *WHO Director-General's opening remarks at the media briefing on COVID-19 - 11 March 2020*. Retrieved July 27, 2021, from https://www.who.int/director-general/speeches/detail/who-director-general-s-opening-remarks-at-the-media-briefing-on-covid-19---11-march-2020

World Health Organization. (2022). *Environmental surveillance for SARS-CoV-2 to complement public health surveillance: Interim guidance, 14 April 2022*. World Health Organization. https://apps.who.int/iris/handle/10665/353158

Wu, F., Zhang, J., Xiao, A., Gu, X., Lee, L., Armas, F., & Kauffman, K. (2020). SARS-CoV-2 titers in wastewater are higher than expected from clinically confirmed cases. *mSystems*, *5*(4), 1–9. https://doi.org/10.1128/mSystems.00614-20

Wurtzer, S., Waldman, P., Levert, M., Cluzel, N., Almayrac, J. L., Charpentier, C., Masnada, S., Gillon-Ritz, M., Mouchel, J. M., Maday, Y., Boni, M., Moulin, L., Marechal, V., Le Guyader, S., Bertrand, I., Gantzer, C., Descamps, D., Charpentier, C., Houhou, N., … Pawlotsky, J. M. (2022). SARS-CoV-2 genome quantification in wastewaters at regional and city scale allows precise monitoring of the whole outbreaks dynamics and variants spreading in the population. *Science of the Total Environment, 810*, 152213. https://doi.org/10.1016/j.scitotenv.2021.152213

Ye, Y., Ellenberg, R. M., Graham, K. E., & Wigginton, K. R. (2016). Survivability, partitioning, and recovery of enveloped viruses in untreated municipal wastewater. *Environmental Science & Technology*, *50*(10), 5077–5085. https://doi.org/10.1021/acs.est.6b00876

Zhang, T., Breitbart, M., Lee, W. H., Run, J. Q., Wei, C. L., Soh, S. W. L., Hibberd, M. L., Liu, E. T., Rohwer, F., & Ruan, Y. (2006). RNA viral community in human feces: Prevalence of plant pathogenic viruses. *PLoS Biology*, *4*(1), 0108–0118. https://doi.org/10.1371/journal.pbio.0040003

Appendices

Appendix A

Supplementary Information

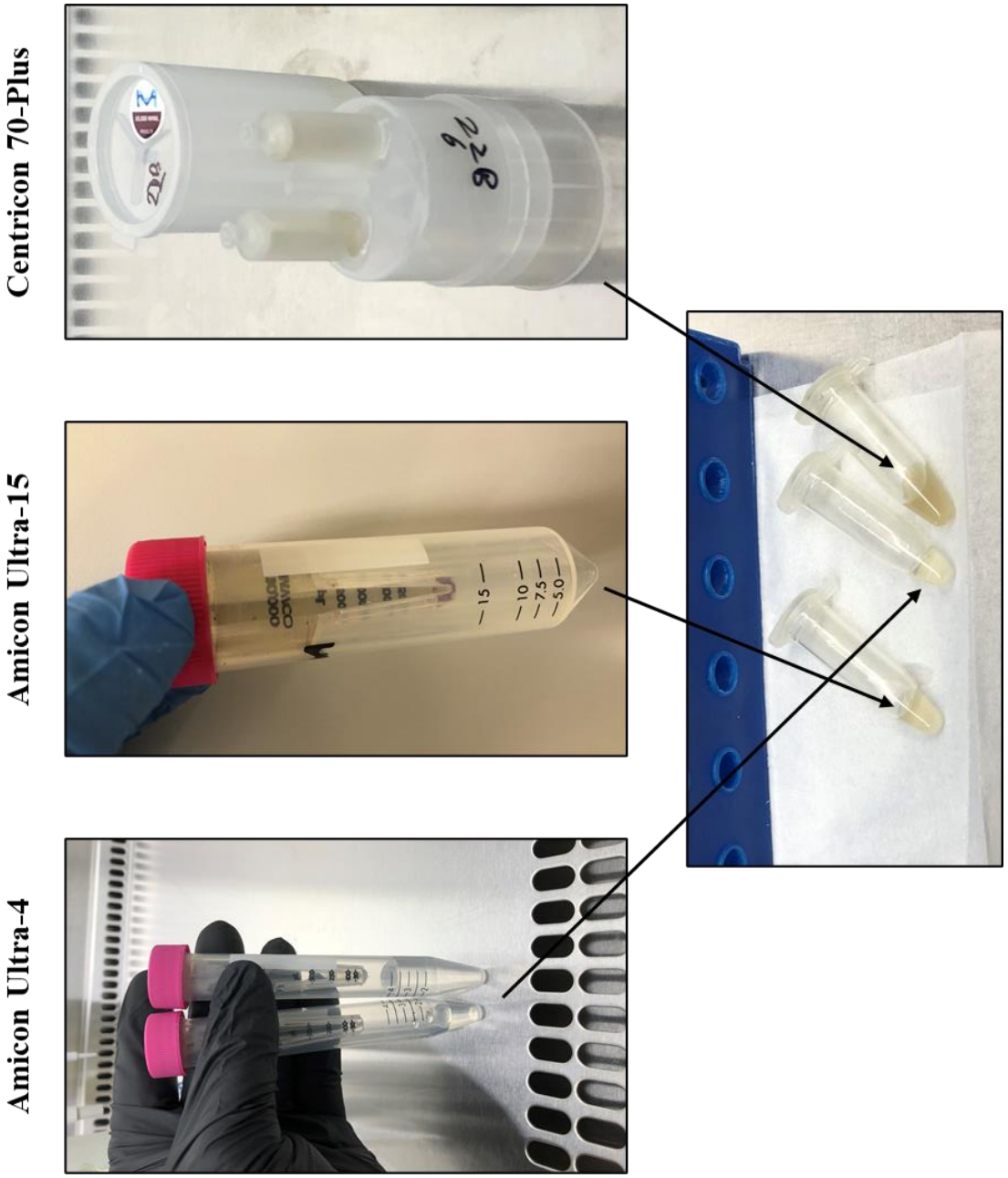

Figure A1. An example of the opacity of concentrates from the three tested ultrafiltration devices in this study.

Table A1. Main specification differences between ultrafiltration devices tested in this study. The details are for the 10 kDa models and extracted from each device's user guide (www.emdmillipore.com).

Ultrafiltration Device	Rotor	Maximum Capacity (mL) [fixed / swing]	Maximum Force (*g*) [fixed / swing]	Concentrate Retrieval	Active Surface Area (cm^2)
Amicon Ultra-4	Fixed / swing	3.5 / 4	4,000 / 7,500	Pipette from the filter device	3.0
Amicon Ultra-15	Fixed / swing	12 / 15	4,000 / 5,000	Pipette from the filter device	7.6
Centricon Plus-70	Swing only	70	3,500	Invert the filter cup, centrifuge, and pipette from the concentration cup	19.0

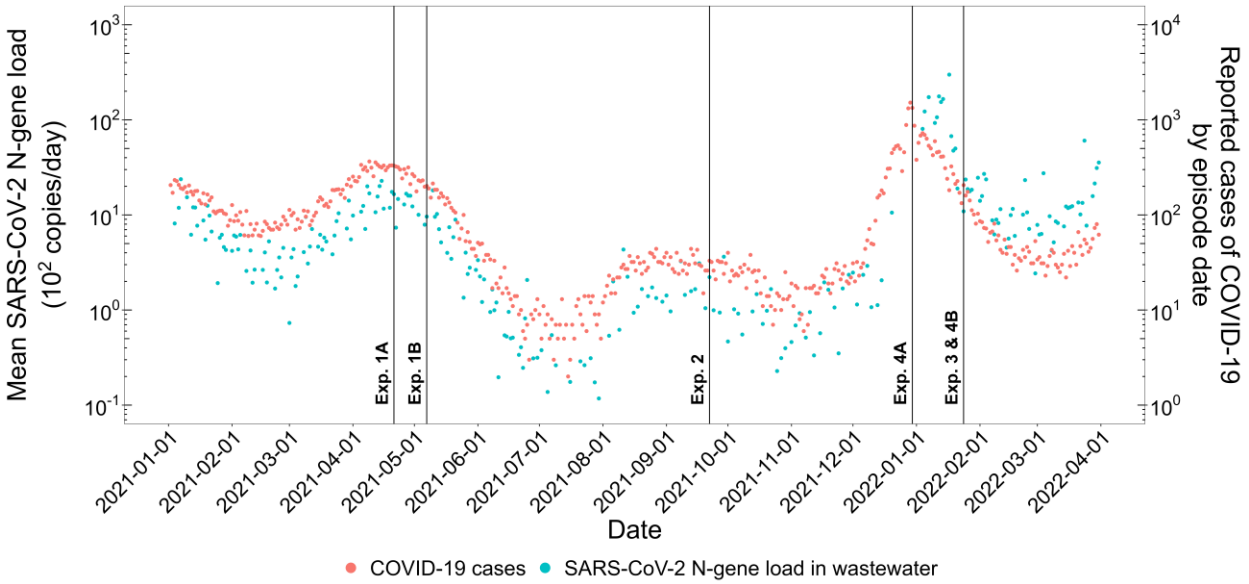

Figure A2. Timeline of when the experiments (1-4) were conducted in this study. The approximate time points (vertical lines) are in reference to SARS-CoV-2 RNA levels in wastewater and COVID-19 clinical cases at the Clarkson wastewater treatment plant, Region of Peel, Canada. The original data was provided by M. Servos (University of Waterloo, personal communication) and is available from the Region of Peel's "Respiratory Viruses" report (https://www.peelregion.ca/coronavirus/case-status/Respiratory-Virus-Activity-Report.pdf).

Table A2. The total amount[a] of RNA for the surrogates (229E, MHV) that were seeded into the wastewater samples. The mean copies of RNA are based on the "spiked extraction blanks" (n = 4) during RNA extraction.

Experiment	Mean log_{10} Copies ± SD 229E	Mean log_{10} Copies ± SD MHV
Experiment 1A[b]	5.45 ± 0.15	5.22 ± 0.15
Experiment 1B[b]	4.83 ± 0.15	4.64 ± 0.06
Experiment 2[b]	5.01 ± 0.06	4.57 ± 0.05
Experiment 3[c]	6.09 ± 0.06	5.15 ± 0.05
Experiment 4A[c]	6.12 ± 0.08	5.33 ± 0.04
Experiment 4B[c]	5.63 ± 0.10	4.90 ± 0.05

Abbreviations: 229E = human coronavirus 229E; MHV = murine hepatitis virus.

[a] Total amount of virus was estimated using the RNeasy PowerMicrobiome Kit[a,b] by seeding both viruses into a blank bead tube (spiked extraction blank).

[b] RNA extraction proceeded as outlined by the main text.

[c] Before 229E and MHV were seeded into the bead tubes, 10 µg of poly(A) (Fisher Scientific, Mississauga, ON, Canada) was added to help carry the viral RNA through the extraction.

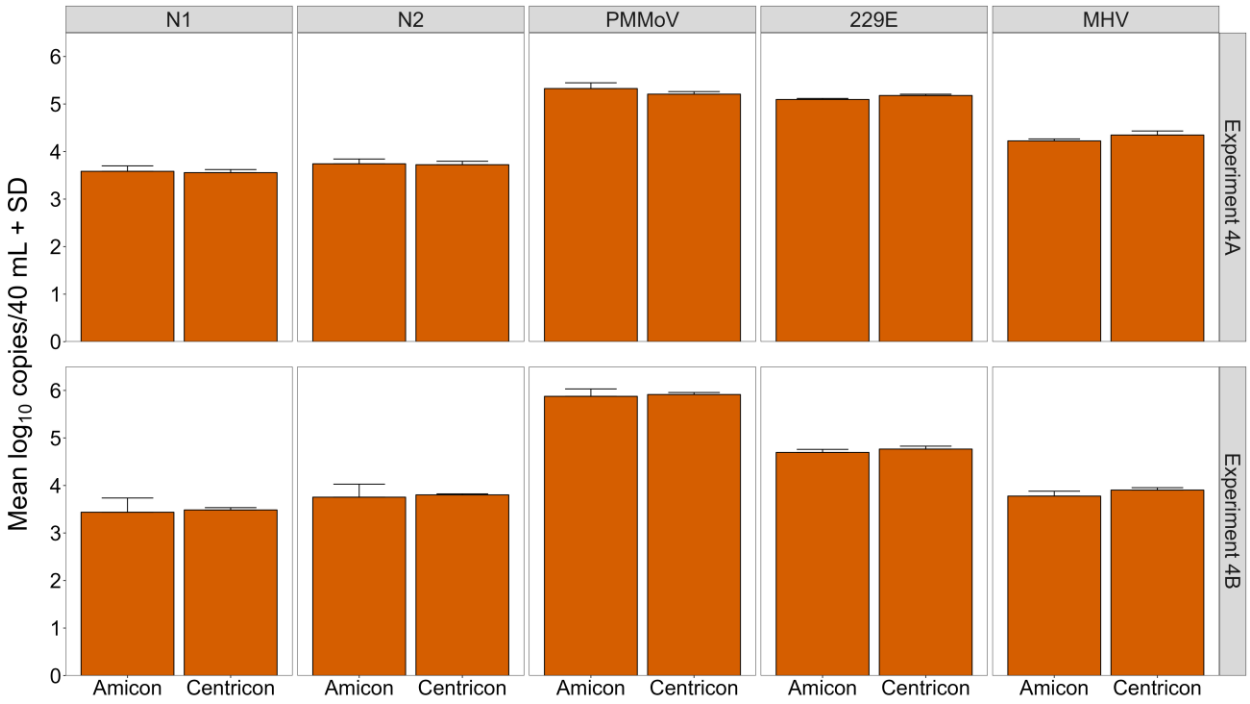

Figure A3. RNA copies per 40 mL of wastewater in the pellet fractions for Experiments 4A/B. There is one pellet fraction represented under "Amicon" as the supernatant from one sample tube was used for both the Amicon Ultra-4 and Ultra-15 devices.

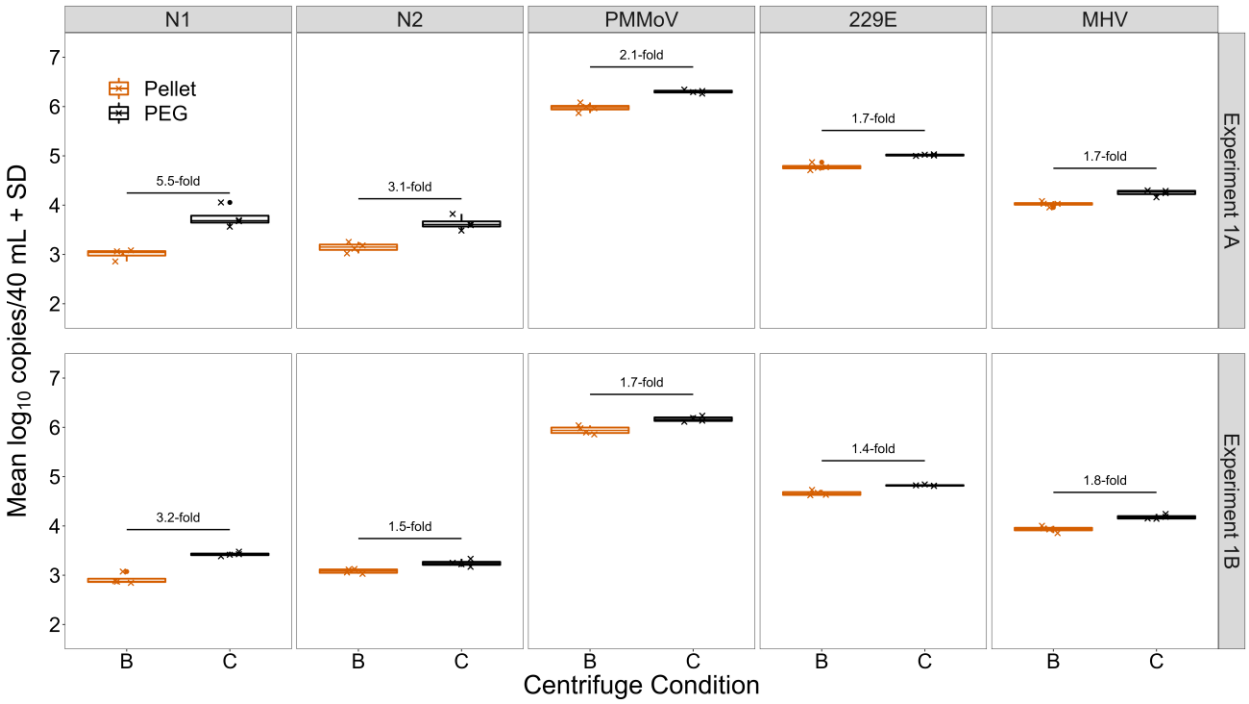

Figure A4. Experiments 1A/B: RNA copies per 40 mL of wastewater without PEG precipitation (Condition B, "Pellet") and with PEG precipitation (Condition C, "PEG") for SARS-CoV-2 (N1 and N2), PMMoV, 229E, and MHV. The presented data is a subset of Experiments 1A/B (Figure 4) as the "Pellet" (solids) and "PEG" (PEG precipitation) treatments. All samples were centrifuged at 12,000 x *g* for 1.5 h and without a brake as used for Conditions B and C.

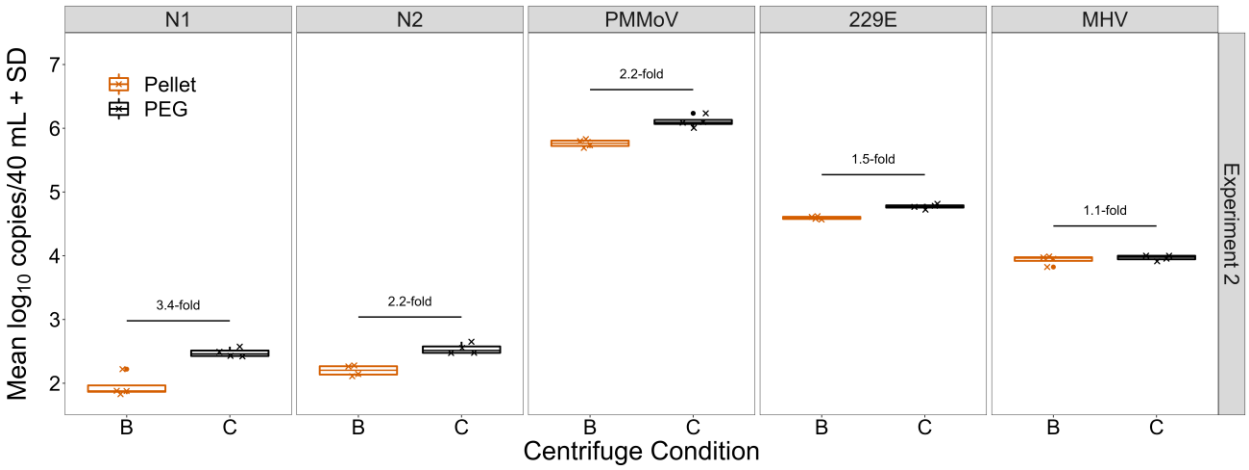

Figure A5. Experiment 2: RNA copies per 40 mL of wastewater without PEG precipitation (Condition B, "Pellet") and with PEG precipitation (Condition C, "PEG") for SARS-CoV-2 (N1 and N2), PMMoV, 229E, and MHV. The presented data is a subset of Experiment 2 (Figure 5) as the "Pellet" (solids) and "PEG" (PEG precipitation) treatments. All samples were centrifuged at 12,000 x *g* for 1.5 h and without a brake as used for Conditions B and C.

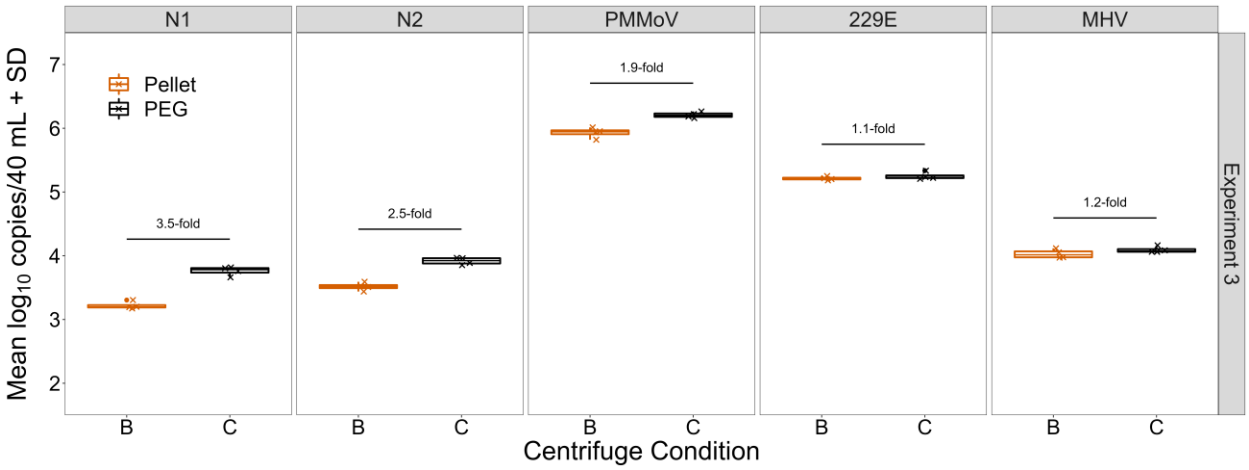

Figure A6. Experiment 3: RNA copies per 40 mL of wastewater without PEG precipitation (Condition B, "Pellet") and with PEG precipitation (Condition C, "PEG") for SARS-CoV-2 (N1 and N2), PMMoV, 229E, and MHV. The presented data is a subset of Experiment 3 (Figure 6) as the "Pellet" (solids) and "PEG" (PEG precipitation) treatments. All samples were centrifuged at 12,000 x *g* for 1.5 h and without a brake as used for Conditions B and C.

Table A3. Comparison of apparent partitioning calculations in terms of copies per 40 mL of wastewater and copies/mass equivalence. The shown values are from a single sample in Experiment 1A under Condition B (12,000 x *g*, 1.5 h, no brake) and reflect the calculation that can be applied to determine the apparent partitioning of viral RNA in wastewater.

Metric	Fraction	Fractional Copies	Total Copies	Apparent Partitioning
Copies/40 mL*	Supernatant (liquid)	938 cp/40 mL	1979 cp/40 mL	47.4%
	Pellet (solids)	1041 cp/40 mL		52.6%
Copies/ME†	Supernatant (liquid)	23 cp/mL (938 cp/40 mL)	4017 cp/ME	0.52%
	Pellet (solids)	4430 cp/g (1041 cp/0.235 g)		99.48%

Abbreviations: cp = copies; ME = mass equivalence.

* Copies/40 mL can be scaled by sample process volume. For example, per 40 mL can be reflected as copies/mL if both fractions are divided by 40.

† Assumes 1 mL of the supernatant = 1 g of the pellet.

Appendix B
Amplification Protocols for 229E and MHV

Amplification protocols for 229E and MHV that were used in this thesis were graciously provided by Ph.D. candidate Scott Joseph Boegel from Dr. Marc Aucoin's lab, University of Waterloo, ON, Canada.

HCoV-229E Amplification Protocol

Human coronavirus 229E (HCoV-229E; ATCC VR-740) was propagated on MRC-5 (ATCC CCL-171) cells (Cedarlane, Burlington, ON, Canada). MRC-5 cells were maintained in Eagle's minimum essential medium (EMEM) supplemented with 10% fetal bovine serum (FBS) by volume (Wisent BioProducts, Saint-Jean-Baptiste, QC, Canada). Cells were serially passaged in tissue culture-treated T-flasks (Thermo Fisher Scientific, Waltham, MA, USA) and incubated at 37°C in a humidified 5% CO_2 in air atmosphere.

MRC-5 cells were seeded to achieve an 80-90% confluent monolayer after 24-48 h, washed with Dulbecco's phosphate buffered saline (D-PBS; Wisent BioProducts), and infected with HCoV-229E at a multiplicity of infection (MOI) of 0.01 in a minimal volume of infection medium (e.g., 2.5 mL in a T-75 flask). After 1 h incubation, additional infection medium was added to reach the normal working volume of the flask (e.g., 10 mL in a T-75 flask); infection medium was EMEM supplemented with 2% FBS by volume. Infected cells were incubated at 34°C in a humidified 5% CO_2 in air atmosphere until cytopathic effects were observed to have progressed through approximately 80% of the monolayer (4-6 days). Culture supernatant was then harvested, centrifuged at 1000 x *g* to remove cells and cell debris, aliquoted, and stored at -80°C until use.

MHV Amplification Protocol

Murine hepatitis virus (ATCC VR-764) was propagated on NCTC clone 1469 cells [derivative of NCTC 721] (ATCC CCL-9.1) (Cedarlane, Burlington, ON, Canada). NCTC 1469 cells were maintained in Dulbecco's Modified Eagle's Medium (DMEM) (Wisent BioProducts, Saint-Jean-Baptiste, QC, Canada) supplemented with 10% horse serum by volume (Sigma-Aldrich, Oakville, ON, Canada). Cells were serially passaged in cell culture treated T-flasks (Thermo Fisher Scientific, Waltham, MA, USA) and incubated at 37°C in a humidified 5% CO_2 in air atmosphere.

For propagation, cells were seeded to achieve an 80-90% confluent monolayer after 24-48h, washed with D-PBS, and infected at a multiplicity of infection (MOI) of 0.01 with a minimal volume of NCTC 135 medium (Sigma-Aldrich). After 1 h incubation at 37°C in a humidified 5% CO_2 in air atmosphere, NCTC 135 supplemented with 10% horse serum by volume was added to reach normal working volume (e.g., 10 mL in a 75 cm^2 tissue culture flask). The flask was then incubated for 24 h at 37°C in a humidified 5% CO_2 in air atmosphere and the supernatant harvested. Supernatant was centrifuged at 1,000 x *g* to remove cells and cell debris and then aliquoted and stored at -80°C until use.

Appendix C

Statistical Analysis

Table C1. Summary of one-way ANOVA results for RNA copies between centrifugal conditions separated by experiment (1-3) and gene target (N1, N2, PMMoV, 229E, MHV). The one-way ANOVA tests were conducted at alpha = 0.05. Additionally, the mean $\log_{10}$ copies per 40 mL of wastewater ± SD are reported with Tukey's post-hoc results shown by a lowercase letter (dissimilar letters indicate significant differences at alpha = 0.05) with all treatments (centrifugal conditions) n = 4.

Experiment	Target	ANOVA Results		Tukey Post-hoc Results	
		F (df)	p	Centrifuge Condition	Mean $\log_{10}$ copies/40 mL ± SD
Experiment 1A	N1	21.8 (4,15)	<0.001	Condition A_SUP	3.37 ± 0.11 c
				Condition A_PEL	2.81 ± 0.10 a
				Condition B_SUP	2.97 ± 0.23 a
				Condition B_PEL	3.01 ± 0.10 a
				Condition C_PEG	3.75 ± 0.21 b
	N2	40.1 (4,15)	<0.001	Condition A_SUP	3.61 ± 0.07 c
				Condition A_PEL	2.93 ± 0.09 a
				Condition B_SUP	3.22 ± 0.07 b
				Condition B_PEL	3.14 ± 0.10 b
				Condition C_PEG	3.63 ± 0.14 c
	PMMoV	192.7 (4,15)	<0.001	Condition A_SUP	6.85 ± 0.04 b
				Condition A_PEL	5.85 ± 0.07 a
				Condition B_SUP	6.72 ± 0.06 b
				Condition B_PEL	5.98 ± 0.09 a
				Condition C_PEG	6.30 ± 0.03 c
	229E	101.1 (4,15)	<0.001	Condition A_SUP	5.45 ± 0.07 d
				Condition A_PEL	4.01 ± 0.16 a

				Condition B_SUP	4.89 ± 0.14 bc
				Condition B_PEL	4.78 ± 0.07 b
				Condition C_PEG	5.02 ± 0.01 c
	MHV	90.1 (4,15)	<0.001	Condition A_SUP	4.69 ± 0.08 d
				Condition A_PEL	3.64 ± 0.11 a
				Condition B_SUP	4.30 ± 0.08 b
				Condition B_PEL	4.02 ± 0.05 c
				Condition C_PEG	4.25 ± 0.06 b
Experiment 1B	N1	5.4 (4,15)	0.007	Condition A_SUP	2.88 ± 0.37 a
				Condition A_PEL	2.71 ± 0.11 a
				Condition B_SUP	2.82 ± 0.35 a
				Condition B_PEL	2.92 ± 0.11 ab
				Condition C_PEG	3.43 ± 0.04 b
	N2	4.2 (4,15)	0.017	Condition A_SUP	3.08 ± 0.26 ab
				Condition A_PEL	2.79 ± 0.08 a
				Condition B_SUP	3.08 ± 0.22 ab
				Condition B_PEL	3.08 ± 0.05 ab
				Condition C_PEG	3.24 ± 0.07 b
	PMMoV	70.1 (4,15)	<0.001	Condition A_SUP	6.45 ± 0.12 b
				Condition A_PEL	5.77 ± 0.06 a
				Condition B_SUP	6.59 ± 0.07 b
				Condition B_PEL	5.94 ± 0.08 a
				Condition C_PEG	6.17 ± 0.05 c
	229E	40.5 (4,15)	<0.001	Condition A_SUP	4.86 ± 0.19 c
				Condition A_PEL	3.96 ± 0.05 a
				Condition B_SUP	4.59 ± 0.16 b

				Condition B_PEL	4.66 ± 0.05 bc
				Condition C_PEG	4.82 ± 0.01 bc
	MHV	17.3 (4,15)	<0.001	Condition A_SUP	4.15 ± 0.18 b
				Condition A_PEL	3.48 ± 0.10 a
				Condition B_SUP	3.99 ± 0.21 b
				Condition B_PEL	3.93 ± 0.06 b
				Condition C_PEG	4.18 ± 0.04 b
Experiment 2	N1	20.6 (2,9)	<0.001	Condition A_PEL	1.75 ± 0.21 a
				Condition B_PEL	1.95 ± 0.18 a
				Condition C_PEG	2.48 ± 0.07 b
	N2	25.7 (2,9)	<0.001	Condition A_PEL	2.03 ± 0.13 a
				Condition B_PEL	2.20 ± 0.08 a
				Condition C_PEG	2.54 ± 0.08 b
	PMMoV	55.0 (4,15)	<0.001	Condition A_SUP	6.13 ± 0.04 b
				Condition A_PEL	5.62 ± 0.03 a
				Condition B_SUP	6.04 ± 0.06 b
				Condition B_PEL	5.76 ± 0.06 c
				Condition C_PEG	6.11 ± 0.09 b
	229E	71.2 (4,15)	<0.001	Condition A_SUP	4.16 ± 0.12 c
				Condition A_PEL	4.63 ± 0.08 a
				Condition B_SUP	3.53 ± 0.22 b
				Condition B_PEL	4.59 ± 0.02 a
				Condition C_PEG	4.77 ± 0.04 a
	MHV	66.2 (4,15)	<0.001	Condition A_SUP	3.20 ± 0.15 c
				Condition A_PEL	3.95 ± 0.03 a
				Condition B_SUP	2.26 ± 0.37 b

				Condition B_PEL	3.93 ± 0.08 a
				Condition C_PEG	3.97 ± 0.04 a
Experiment 3	N1	29.1 (4,15)	<0.001	Condition A_SUP	3.42 ± 0.09 b
				Condition A_PEL	3.01 ± 0.19 a
				Condition B_SUP	3.24 ± 0.05 b
				Condition B_PEL	3.22 ± 0.06 ab
				Condition C_PEG	3.76 ± 0.07 c
	N2	15.7 (4,15)	<0.001	Condition A_SUP	3.68 ± 0.06 b
				Condition A_PEL	3.35 ± 0.22 a
				Condition B_SUP	3.47 ± 0.05 ab
				Condition B_PEL	3.52 ± 0.06 ab
				Condition C_PEG	3.92 ± 0.06 c
	PMMoV	54.3 (4,15)	<0.001	Condition A_SUP	6.46 ± 0.08 b
				Condition A_PEL	5.80 ± 0.13 a
				Condition B_SUP	6.49 ± 0.06 b
				Condition B_PEL	5.93 ± 0.08 a
				Condition C_PEG	6.21 ± 0.05 c
	229E	106.0 (4,15)	<0.001	Condition A_SUP	5.25 ± 0.07 c
				Condition A_PEL	4.64 ± 0.02 a
				Condition B_SUP	5.00 ± 0.06 b
				Condition B_PEL	5.21 ± 0.03 c
				Condition C_PEG	5.25 ± 0.06 c
	MHV	34.0 (4,15)	<0.001	Condition A_SUP	3.89 ± 0.12 c
				Condition A_PEL	3.70 ± 0.02 a
				Condition B_SUP	3.64 ± 0.03 a
				Condition B_PEL	4.03 ± 0.07 bc

	Condition C_PEG	4.09 ± 0.05 b

Conditions:
Condition A (4,000 x *g*, 10 min, with brake).
Condition B (12,000 x *g*, 1.5 h, no brake).
Condition C (overnight PEG precipitation followed by centrifugation at 12,000 x *g* for 1.5 h without a brake).
Fractions:
SUP = supernatant.
PEL = pellet.
PEG = PEG (polyethylene glycol) precipitation/centrifugation.

Table C2. Summary of one-way ANOVA results for RNA copies between ultrafiltration devices separated by experiment (4A/B) and gene target (N1, N2, PMMoV, 229E, MHV). The one-way ANOVA tests were conducted at alpha = 0.05. Additionally, the mean $\log_{10}$ copies per 40 mL of wastewater ± SD are reported with Tukey's post-hoc results shown by a lowercase letter (dissimilar letters indicate significant differences at alpha = 0.05) with all treatments (ultrafiltration devices) n = 4.

		ANOVA Results		Tukey Post-hoc Results	
Experiment	**Target**	**F (df)**	**p**	**Ultrafiltration Device**	**Mean log10 copies/40 mL ± SD**
Experiment 4A	N1	121.0 (2,9)	<0.001	Amicon Ultra-4	3.26 ± 0.09 c
				Amicon Ultra-15	2.50 ± 0.05 a
				Centricon Plus-70	3.46 ± 0.12 b
	N2	36.8 (2,9)	<0.001	Amicon Ultra-4	3.51 ± 0.14 b
				Amicon Ultra-15	2.79 ± 0.13 a
				Centricon Plus-70	3.65 ± 0.18 b
	PMMoV	279.3 (2,9)	<0.001	Amicon Ultra-4	5.83 ± 0.08 b
				Amicon Ultra-15	4.98 ± 0.06 a
				Centricon Plus-70	5.90 ± 0.03 b
	229E	73.6 (2,9)	<0.001	Amicon Ultra-4	4.73 ± 0.13 c
				Amicon Ultra-15	4.06 ± 0.09 a
				Centricon Plus-70	5.01 ± 0.12 b
	MHV	36.2 (2,9)	<0.001	Amicon Ultra-4	3.54 ± 0.19 b
				Amicon Ultra-15	2.89 ± 0.12 a
				Centricon Plus-70	3.86 ± 0.18 b
Experiment 4B	N1	88.1 (2,9)	<0.001	Amicon Ultra-4	3.05 ± 0.11 c
				Amicon Ultra-15	2.53 ± 0.13 a
				Centricon Plus-70	3.54 ± 0.07 b
	N2	39.2 (2,9)	<0.001	Amicon Ultra-4	3.44 ± 0.10 c

				Amicon Ultra-15	3.05 ± 0.08 a
				Centricon Plus-70	3.71 ± 0.12 b
	PMMoV	35.5 (2,9)	<0.001	Amicon Ultra-4	6.37 ± 0.05 b
				Amicon Ultra-15	6.00 ± 0.03 a
				Centricon Plus-70	6.42 ± 0.12 b
	229E	55.2 (2,9)	<0.001	Amicon Ultra-4	4.36 ± 0.13 c
				Amicon Ultra-15	3.84 ± 0.11 a
				Centricon Plus-70	4.60 ± 0.06 b
	MHV	37.8 (2,9)	<0.001	Amicon Ultra-4	3.35 ± 0.15 c
				Amicon Ultra-15	2.80 ± 0.17 a
				Centricon Plus-70	3.62 ± 0.06 b